# Report from the Hotspot Geodynamics Detailed Planning Group

*R. Duncan, College of Oceanic and Atmospheric Sciences, Oregon State University, USA*
*N. Arndt, LGCA, University Joseph Fournier-Grenoble, France*
*T. Hanyu, Institute for Research on Earth Evolution, JAMSTEC, Japan*
*Y. Harada, Tokai University, Japan*
*K. Harpp, Department of Geology, Colgate University, USA*
*K. Hoernle, IFM-GEOMAR, Universitat Christian-Albrechts, Kiel, Germany*
*L. Kellogg, Department of Geology, University of California, Davis, USA*
*D. Kent, Department of Geological Sciences, Rutgers University, USA*
*A. Koppers, IGPP-SIO, University of California, San Diego, USA*
*W. Sager, Department of Oceanography, Texas A&M University, USA*
*B. Steinberger, Sentrum for Geodynamikk, Norges Geologiske Undersøkelse, Norway*
*J. Tarduno, Department of Earth and Environmental Sciences, University of Rochester, USA*
*Y.-G. Xu, CAS Institute of geochemistry, Guangzhou University, China*

(*Resulting from a meeting at University of Hawaii, Manoa, January 12-13, 2007*)

## I. CURRENT ISSUES IN HOTSPOT GEODYNAMICS

### 1. Introduction

Volcanic chains associated with deep-seated mantle plumes potentially provide valuable information on mantle geodynamics and geochemistry, in particular in establishing the timing and magnitude of plume motion, the timing and magnitude of whole Earth motion with respect to the spin axis ("true polar wander"), and plume-lithosphere interaction. Drilling and post-cruise studies associated with ODP Leg 197 demonstrated that the Hawaiian hotspot drifted south, from ~35°N to 20°N between 80 and 49 Ma (Tarduno et al., 2003). The direction and magnitude of this observed hotspot drift is in accord with recent modeling of plume advection in a whole mantle convective regime (Steinberger et al., 2004). Uncertainties in the paleomagnetically-determined paleolatitudes and the predicted hotspot drift leave open the possibility that some of the southward motion could be due to whole Earth motion (Goldreich and Toomre, 1969). Three current IODP proposals (620-Full3, 636-Full2, 669-Pre) focus on drilling hotspot chains to address themes including hotspot motion, the temporal evolution of hotspot mantle sources, plate motion reference frames, and mantle plume models. A detailed planning group (DPG) was commissioned by the Science Planning Committee (SPC) to review current information, methods and models, and to develop an optimal global drilling plan (including drilling, logging and post-cruise science) to address:

**1.** The minimal/optimal paleomagnetic observations necessary to distinguish whole Earth motion ("true polar wander") from hotspot drift; that is, the number and location of sites within an ocean basin; the number and location of seamount chains among several ocean basins; the most appropriate order of drilling.
**2.** Geochemical parameters that are available for discriminating between deep plumes vs. shallow plumes or no plumes; geochemical estimates of mantle potential temperatures; the

minimal/optimal drilling strategy for assessing the geochemical evolution of seamounts, and systematic source variability along lineaments.
**3.** The improvements in mantle flow models afforded by seamount paleolatitudes, and through them determination of timing, direction and magnitude of hotspot drift.
**4.** The best strategy to obtain robust paleolatitude estimates from a single seamount; depth of penetration and number of independent cooling units flows needed to average secular variation.
**5.** Integration of independent types of paleolatitude information (e.g., continental apparent polar wander paths, sediment paleoequator, skewness of seafloor magnetic anomalies, seamount paleopoles) to better estimate whole Earth motion.

This report is the outcome of written contributions, presentations and discussions at the University of Hawaii, January 12-13, 2007. All members of the DPG participated in the writing and editing of this consensus view.

## 2. Scientific Results from ODP Leg 197 – Motion of the Hawaiian Hotspot

The bend in the Hawaiian-Emperor volcanic chain is an often-cited example of a change in plate motion with respect to a stationary hotspot. Growing evidence, however, suggests that the bend might instead record variable drift of the Hawaiian hotspot within a convecting mantle (Figure 1). Paleomagnetic and radiometric age data from samples recovered during Ocean Drilling Program (ODP) Leg 197 (and Suiko seamount, DSDP Site 433) define an age-progressive paleolatitude history (Figure 2), indicating that the Emperor Seamounts volcanic trend was formed principally by rapid (4-5 cm/yr) southward motion of the Hawaiian hotspot during Late Cretaceous to early Tertiary time (81 to 49 Ma). The age-distance relationship among the seamounts also indicate variations in Pacific plate velocity during this period (Figure 3).

Petrochemical data and observations of volcanic products (lava flows and volcaniclastic sediments) from Detroit, Suiko, Nintoku, and Koko seamounts provide records of the evolution of these volcanic systems for comparison with recent activity in the Hawaiian Islands. The Emperor Seamounts formed from similar mantle sources (plume components and lithosphere), with the same stages of volcanic activity and time span as the Hawaiian volcanoes. Changes in major and trace element, and Sr isotopic compositions of shield lavas along the lineament can be related to variations in thickness of the lithosphere overlying the hotspot, that control the depth and extent of partial melting. Other geochemical tracers, such as He, Pb and Hf isotopic compositions, indicate persistent contributions to melting from the plume throughout the volcanic chain (Figure 4).

## 3. Hotspot motions predicted from large-scale mantle flow models

Modeled hotspot motions in the interval 100-0 Ma for Hawaii, Louisville, Easter, Kerguelen, Reunion, Tristan, and Iceland hotspots, and their sensitivity to various model parameters (mantle viscosity structure, plume startup age, plume rise height, etc.) have been described in a number of papers by Steinberger and co-authors (starting with Steinberger and O'Connell, 1998). These models first compute the large-scale mantle flow field from internal density

heterogeneities (as inferred from seismic tomography studies), the viscosity structure of the mantle and plate motions. Plume conduits are inserted into this flow field. They are assumed initially vertical, but which subsequently tilt as they are advected into the large-scale flow field. The conduit sources are assumed to move with the horizontal flow at the source depth (lowermost mantle) or, alternatively, to be fixed. This depth is greater for older plume initiation ages, or when the plume has a larger buoyancy flux (corresponding to faster plume rising speed). Hotspot motion, for the first few million years, follows flow in the upper mantle. Under fast moving plates, this tends to be in the direction of plate motion. After a steady-state tilt has been established in the upper mantle, hotspot motion then tends to reflect flow at the source depth in the lower mantle (Figures 5, 6). This depth is greater for older plume initiation ages, or when the plume has a larger buoyancy flux (corresponding to faster plume rise velocity).

Uncertainties in the amount of hotspot motion come from (a) the tomographic model used to compute large-scale flow (these differ in magnitude, but not so much in the large-scale pattern), (b) the conversion factor used to calculate density from seismic velocity, and (c) the viscosity model (with higher viscosities corresponding to slower flow). Some models with reasonable input parameters can produce unrealistically large hotspot motions, particularly when a tilted conduit rises upward through the upper mantle causing hotpot motion to exceed the large-scale mantle flow. Directions of hotspot motion, on the other hand, are more reliably predicted than magnitudes, at least for those hotspots where a large motion is predicted. For a number of hotspots (e.g., Easter, Tristan, Kerguelen), the interpretation of hotspot chains is complicated because of possible effects of plume-ridge interaction. Summaries of model results for individual hotspots are:

*Hawaii:*
A robust feature of virtually all model runs is a south-southeastward hotspot motion (e.g., Figure 1). The magnitude of hotspot motion during the past 100 Ma, however, varies between a few 100 km and more than 1000 km depending mostly on the plume initiation age, which is unknown because the end of the hotspot track has been subducted. Since constraints on latitude shift exist (Tarduno et al., 2003), the model can be calibrated to approximately match the latitudinal motion by choosing a suitable plume initiation age. It is difficult, though, to obtain a model where latitude shift occurs mainly during the formation of the Emperor chain, and no model can produce a latitudinal motion that stops abruptly at the time of the Hawaiian-Emperor bend.

*Louisville:*
An overall feature of most model results is an average slow eastward or southeastward hotspot motion of the Louisville hotspot since about 78 Ma (Figure 6). However, the predicted amount of motion tends to be much smaller than for the Hawaiian hotspot, typically not more than a few hundred km. Based on the modeling results, large changes in latitude (of the magnitude observed for the Emperor chain during the same time span) are not expected, in contrast with the rather large (~25°) southward motion needed to reconcile the paleolatitude of Ontong Java plateau with the present location of the hotspot (Antretter et al., 2004).

*Kerguelen:*
Whereas earlier models yielded a southeastward motion of the Kerguelen hotspot, which is compatible with existing paleolatitude data and geometry of the Ninetyeast ridge (Antretter et al., 2002), the latest model results are in contrast (Figure 6). Flow direction changes with depth and the newer model reflects "deeper" flow because of more massive plumes. Hence, the newer results agree less well with observations. Kerguelen is really the only hotspot for which the latest modeling results are substantially different from older ones. Ocean floor age changes across the Ninetyeast ridge, corresponding to fracture zones at and near the eastern edge of ridge (Müller et al., 1997). The predicted Kerguelen track age on the Indian plate is always approximately the same as the underlying ocean floor age, which could indicate that the Ninetyeast ridge did not form directly above the hotspot, but rather at the location along the spreading ridge/transform fault closest to the hotspot.

*Reunion:*
Most models agree that the Reunion hotspot (from 65 Ma) drifted only a few 100 km northward, corresponding to the initially vertical conduit being tilted over by the fast moving Indian plate, followed by slow ~eastward motion (not more than a few 100 km) for the rest of the plume lifespan. Plate motion models (Müller et al., 1997) indicate similar hotspot track and seafloor age over the early history of the plume, so that the Indian plate part of the hotspot track may have formed at the spreading ridge rather than directly above the plume.

*Tristan:*
Most modeling results agree on slow (not more than a few 100 km) hotspot motion in a southwesterly to southeasterly direction over the past 100 Ma, with some models showing almost no hotspot motion; the latest models indicate more southwesterly motion, corresponding to flow deeper in the mantle. Plate motion modeling (Muller et al., 1997) indicates close proximity between plume and spreading ridge before about 80 Ma.

*Other points:*
While paleomagnetically-derived paleolatitudes on hotspot tracks offer the most direct test of hotspot motion, other estimates of paleolatitudes (apparent polar wander paths derived from continental regions of plates, skewness of marine magnetic anomalies, paleoequator sediment bulge) can be utilized. Formal uncertainties of modeled hotspot motion are difficult to quantify, but progress has been made with quantifying uncertainties of plate motions relative to (fixed or moving) hotspot reference frames, based solely on the uncertainties of data (i.e., ages and localities of hotspot volcanism). Methods to deal with such uncertainties are developed in O'Neill et al. (2005), Wessel et al. (2006), and Kirkwood et al. (1999).

## 4. Geochronology of Hotspot Chains

Knowledge of the timescale for construction of individual seamounts and the overall age distribution of seamount trails are key requirements for answering important geodynamical questions with regard to hotspots. Placing the samples used for performing paleomagnetic and geochemical measurements in a solid temporal framework, with high-precision $^{40}$Ar-$^{39}$Ar age

determinations, provides basic information for addressing themes of hotspot motion, temporal evolution of hotspot mantle sources, plate-motion reference frames and mantle plume models.

The orientation and age progression in volcano construction along island and seamount trails form the basis for the hotspot frame of reference. This database has been used to promote the "fixed" hotspot hypothesis (Morgan 1972a; 1972b; 1981; Duncan and McDougall, 1976; Duncan, 1981; Duncan and Clague, 1985). The Hawaiian and Louisville seamount trails have been used as key hotspot examples, because both have simple geometries and depicted linear age progressions over an interval approaching 80 m.y. (Dalrymple and Clague 1976; Dalrymple *et al.* 1977; Duncan and Clague 1985; Watts *et al.* 1988). However, this simple picture is now being revised with more precise and accurate measurements using modern $^{40}$Ar-$^{39}$Ar age determinations, using incremental heating experiments on mineral separates and groundmass (Duncan and Keller 2004; Koppers *et al.* 2004; Sharp and Clague 2006). These measurements show that the age progressions are not linear after all, that the measured velocities vary considerably along these seamount trails, and that inter-hotspot motion, together with Pacific plate motion, is required to successfully model the volcanic chains (Duncan and Keller 2004; Koppers *et al.* 2004; Figures 3, 7).

Geochronological data have revealed that intraplate seamounts have taken several million years to form, from their rapidly-erupted, voluminous shield-building stage to the last intermittent eruptions during the post-erosional stage (Clague and Dalrymple, 1987). The morphology and longevity of volcanic activity of seamount trails close to spreading ridges appears to be strongly influenced by the broad shallow mantle upwelling. These observations refine our views of how seamount trails are formed and how hotspots (plumes) themselves move and interact with the lithosphere. Plate motions may still be constrained from hotspot trails, but in addition to age progressions and trail morphologies we must incorporate possible motion of plumes and communication with nearby spreading ridges. High precision $^{40}$Ar-$^{39}$Ar age determinations provide an important tool in deciphering these cases.

*Measurement and Drilling Requirements*

To get reliable crystallization ages suitable for distinguishing plate from hotspot motion through ocean drilling of seamount trails, two issues need to be addressed. First, the drilling should be deep enough to circumvent any substantial seawater alteration, which can hamper age determinations of dredge samples. Experiences with previous drilling legs show that drilling more than 20 m into the volcanic basement should be sufficient to retrieve relatively fresh basaltic samples for age studies. Samples to be used for $^{40}$Ar-$^{39}$Ar age determinations should have either holocrystalline groundmasses (i.e. devoid of any devitrified basaltic glass), unaltered plagioclase, hornblende or biotite phenocrysts, or have relatively high potassium abundances (Koppers *et al.* 2000; 2004; Figure 8). These considerations support recovery of multiple lava flows, through deep penetration (>100 m).

Second, drilling should be designed to sample key phases of the volcanic history at each location along the seamount trails. For plate and hotspot motion reconstructions it is important to know the age of the shield-building stage, whereas to understand the geochemical evolution of the seamounts, the ages of the capping stage and post-erosional volcanism are of importance

as well. This requires drilling at least one deep penetration site per seamount, supplemented with dredging (e.g., from site surveys).

Seamount trails may contain tens or hundreds of individual volcanic edifices, while only a few of these can be sampled by IODP drilling. Dredging other seamounts adjoining the IODP drill sites will provide a better control on the overall age systematics of hotspot trails. Dredging will also provide additional samples from the post-erosional and shield-capping stages, when placed shallow on the top of seamounts or on late volcanic cones. Alternatively, they may sample the early shield-building stages, when placed deep (up to 5-6 km) on the seamount flanks or at the foot of major volcanic rift zones, a depth that normally is unattainable by ocean drilling.

## 5. Plate Apparent Polar Wander Paths

Plate apparent polar wander paths (APWPs) provide a tectonic framework for understanding hotspot motion. Hotspot tracks and paleomagnetic data are two widely used reference frames and comparisons of the two have the potential to illuminate hotspot motion, whole Earth motion, and time-varying non-dipole geomagnetic field components. APWPs can be grouped into two classes: those constructed from continental plates and those from oceanic plates. In practice, this means the continents and the Pacific plate because the latter is the only oceanic plate with a significant amount of paleomagnetic data.

*Continental Plate APWPs*

Paleomagnetic data used for calculating continental plate APWPs are usually measured from fully oriented samples collected from land and are relatively plentiful in number. Data are culled using reliability criteria (e.g., Van der Voo, 1993), grouped by plate, and average poles are usually calculated using data within a time-window (10-20 m.y.) and standard Fisher averaging. The number of data within an age window for a given plate is highly variable. Those from North America and Europe (the most heavily studied plates) tend to have larger numbers of data (in the Besse and Courtillot (2002) compilation, for example, between 50-70 Ma, N=7 for North America and N=11 for Europe). In contrast, plates with sparse data (e.g., Antarctica) often have few or even no data within some time windows. To overcome this irregularity and to make more robust APWP estimates, some studies have used relative plate motion models to reconstruct paleomagnetic data into a single plate reference frame (usually Africa owing to its central position in Pangea reconstructions) and combine data to compute a global, composite APWP (Torsvik and Van der Voo, 2002; Besse and Courtillot, 2002; Schettino and Scotese, 2005; Figure 9). For example, in the same 50-70 Ma time window mentioned above, the Besse and Courtillot (2002) global average pole was determined from N=45 data. As a result of the large number of data, the uncertainty limits are compact ($\alpha_{95}$ = 2.8°).

Although global APWPs are useful for tectonic studies, they have several drawbacks that must be considered when making tectonic interpretations. Different data filtering criteria lead to differences among global APWPs. Numbers of data within given age windows are still small enough that choices about which data to retain can have significant effects. Global

APWPs usually have similar shapes, but differences of 5°-10° scale between coeval poles are common (Figure 9) and this can make for differences in interpretations. For example, Prévot et al. (2000) analyzed only igneous rock data and concluded that there were two large whole Earth motion events during the Mid-Cretaceous, whereas Besse and Courtillot (2002) included sediment data and did not find the same shifts. Furthermore, averaging methods lead to differences among APWPs and may mask some features. Many APWPs were determined with large age windows (up to 20 m.y.) that are often overlapping (meaning that adjacent points are not independent). The large window size and overlapping intervals make for smoother, more regular APWPs, but may mask or subdue important details. Some authors have used spline fits or small circle (Euler pole) fits to further smooth their results (Acton, 1999; Schettino and Scotese, 2005).

Other problems arise from the accuracy of assumptions about sample fidelity and geomagnetic field shape. APWPs that include sedimentary paleomagnetic data (most do) may have inaccuracies caused by inclination error, which is a shallowing of paleomagnetic inclination thought to result from sediment compaction (Anson and Kodama, 1987). Although efforts have been made to develop methods of detecting and correcting for inclination error (e.g., Hodych et al., 1999), these methods have not been widely applied and it is usually uncertain which sediments give accurate results and which are biased. Paleomagnetic poles may also be inaccurate because the assumed shape of the geomagnetic field is incorrect. Most APWP compilations assume that the time-averaged field is that of a geocentric axial dipole. Although many studies have affirmed that this is a good first order approximation (Merrill and McFadden, 2003), other studies have found that small (5-10%), zonal non-dipole fields remain after averaging (McElhinny et al., 1996; Merrill et al., 1996; Torsvik and Van der Voo, 2002). If the persistent non-dipole fields are small, the error in paleolatitude is also small (about 2° for 5% non-dipole field). If such fields were larger, or changed over time, the result could be polar motion that can be misinterpreted as plate motion. Unfortunately, the history of non-dipole field components is highly uncertain, so it is difficult to make corrections, although initial steps are being taken (Torsvik and Van der Voo, 2002).

Inferences of hotspot motion made from APWPs suffer from additional uncertainties. To determine the paleolatitude of a hotspot, the distance from a hotspot seamount to the coeval paleomagnetic pole is calculated (Figure 10). This requires that the age of a seamount is accurately known or can be predicted from a model of hotspot motion. Age is often the largest uncertainty in models of plate motion relative to the hotspots (e.g., Wessel et al., 2006). Moreover, hotspots may be mis-located as a result of plume flow toward ridges. Such cases, however, may be evaluated through use of geochemical tracers of plume-ridge interaction. This is why direct drilling and combining geochemical with paleomagnetic measurements from hotspot seamount chains are invaluable.

The current state of continental APWPs is that several composite paths have been constructed in recent years, each from hundreds of individual data points (Torsvik and Van der Voo, 2002; Besse and Courtillot, 2002; Schettino and Scotese, 2005). Despite small differences in data analysis, the global composite APWPs are very similar, with only small differences in detail. Analysis will continue to improve the reliability of the calculations, but improvements should be incremental because the addition of new data does not increase the number of

samples substantially. It is likely that future improvements will amount to only small changes (<10°) in average pole positions.

*Oceanic plate APWPs*

APWPs for oceanic plates have most of the same drawbacks as continental plates, with the added problem of sparse, sometimes inaccurate, and conflicting data. The big difference is that oceanic plates are difficult to sample and fully-oriented sample data are rare. As a result, oceanic plate APWPs are constructed primarily from magnetic anomaly studies and azimuthally-unoriented core sample analyses (Gordon and Cox, 1980). Each type of data has some drawback, making the delineation of ocean plate APWPs problematic.

Magnetic anomaly data are of two types: inversions of seamount magnetic anomaly data with bathymetry to produce a mean magnetization direction (Richards et al., 1967) and analyses of the skewness (asymmetry) of marine magnetic lineations to determine the effective paleomagnetic inclination (Schouten and Cande, 1976). Seamount data were initially the main constraint for the Pacific plate APWP because they were available when other data were sparse. But this method assumes that the average magnetization is homogeneous and entirely remanent, whereas most seamounts probably have some degree of mixed polarity and magnetic intensity inhomogeneity, and spurious, overprint magnetization. As a result, seamount paleomagnetic poles are inadequate by themselves for detailed tectonic studies. An added limitation is that the age of a given seamount is usually poorly determined.

Magnetic lineation skewness can be investigated with much greater age precision because the anomaly ages are known from the geomagnetic polarity reversal time scale. The main difficulty with skewness data is that they must often be corrected by adding a factor known as "anomalous skewness". Although anomalous skewness can be estimated empirically (Petronotis et al., 1992), the cause of this bias factor is poorly understood. In addition, many Pacific plate skewness data do not match up with other, coeval data, suggesting data inaccuracies.

Core samples are not being azimuthally-oriented, so only paleoinclination (not declination) can be determined from a core. If data from many cores are combined, mean APWP pole positions can be determined (Figure 11); although, the lack of declination data often means pole uncertainties are large in the direction perpendicular to a line connecting the sites and pole (Cox and Gordon, 1984). This problem has been addressed by using declinations from seamount magnetic anomaly models azimuthal constraint (Sager, 2006). Sediment cores also have the problem of a potential inclination error and have been excluded from some studies as a result (Tarduno, 1990). Samples from igneous cores are often considered the most reliable, but have the problem that few holes sample enough statistically-independent cooling units to properly average secular variation and give useful uncertainties (Cox and Gordon, 1984).

The Pacific plate is the only oceanic plate with a reasonably well-determined APWP (Figure 12). The Pacific APWP has changed significantly over the past decade with the calculation of new paleomagnetic poles using core data from the Ocean Drilling Program. Of particular note, the accepted 80 Ma pole is now ~12° farther north than previously determined

(Tarduno and Cottrell, 1997; Cottrell and Tarduno, 2003; Sager, 2006) and disagrees substantially with the amount of northward plate motion implied from fixed hotspot models (Sager, 2007). In contrast, paleomagnetic data for the past 49 Ma are in agreement with fixed hotspot models. Comparison of the APWP with models of older hotspot tracks are complicated by poor definition of the APWP before 123 Ma and uncertain connections of seamount chains older than 80 Ma with the younger hotspot record (Koppers et al., 2003; Wessel et al., 2006). Although the current Pacific APWP seems reasonably well constrained, there are discrepancies that require more study. Magnetic anomaly skewness poles for Late Cretaceous time diverge from other data for unknown reasons. Furthermore, Jurassic and Early Cretaceous anomaly skewness give drastically different APWP depending on whether anomalous skewness is factored in (Larson and Sager, 1992). In addition, data from Ontong Java Plateau seem to depart from the Pacific APWP and may indicate that the plateau (and by implication other parts of the plate) had separate plate motion history (Sager, 2006; 2007).

**6. Mantle Source Heterogeneity and Geochemical Evolution of Hotspot Chains**

Geochemical studies of hotspot chains can resolve several important issues in hotspot and plume dynamics: (1) identifying mantle source components for melting, (2) understanding when and how those components were produced and distributed through the mantle, (3) determining where and at what depth they exist, (4) measuring the scale of heterogeneity in the mantle, and (5) describing the pattern of convection and mantle recycling.

Volcanic rocks in a single hotspot chain, or even in a single volcanic center, show compositional variability, suggesting that mantle plumes include several (end-member) components. For instance, the thick sequence of lava flows and hyaloclastites sampled by the Hawaiian Scientific Drilling Project has produced evidence that the Hawaiian plume involves at least three components (a primitive source, recycled oceanic crust, an EM1-like component, and/or another depleted component) (Bryce et al., 2005; De Paolo et al., 2001; Eisele et al., 2003; Lassiter and Hauri, 1998; Stolper et al., 1996). The degree of melting of each component and mixing ratios among components depend on thermal conditions and structure across the plume, which leads to temporal and spatial geochemical variation in magmas now sampled as lava flows (De Paolo et al., 2001; Ribe and Christensen, 1999). Other hotspots with smaller buoyancy flux or lower potential temperature than Hawaii may exhibit different end-member components (e.g., EM2, HIMU), or different proportions of components in melting. Smaller buoyancy flux hotspots may more clearly demonstrate source compositional heterogeneities than Hawaii because lower degrees of melting produce less homogenization of components.

Geochemical variability intrinsic to the plume may be masked by mixing with lithospheric mantle in intraplate settings, or with upper mantle (asthenosphere) near spreading ridges. For example, growth of Hawaiian volcanoes follows a common evolution from shield-building stage to post-shield stage to post-erosional stage. Increasing contribution of lithospheric mantle to plume melts changes the magma compositions in the course of volcano construction. Current evidence shows a strong contrast between the Hawaiian volcanoes and those in the Louisville chain, where magmas have been very similar over 76 Myr of hotspot activity (Cheng et al, 1987; Hawkins et al, 1987), suggesting a rather constant contribution of the plume. For maximum information about plume composition, drilling should be targeted to

sample the shield-building stage. In hotspot chains with a long history of hotspot-ridge interaction (e.g., Walvis Ridge), plume components may be more difficult to distinguish.

Determining the depth of origin of mantle plumes is difficult to address from geochemical data. However, recently developed tracers, such as Hf-W and Pt-Os isotopic systems, have the potential to identify plumes derived from the core-mantle boundary. The short-lived nuclide, $^{182}$Hf decays to $^{182}$W. Since Hf/W ratios were highly fractionated during core formation, mantle and core should have distinct $^{182}$W/$^{184}$W isotope ratios (Kleine et al, 2002). $^{190}$Pt is a long-lived radionuclide that decays to $^{186}$Os. Pt/Os ratios in the outer core are considered to be elevated in the course of inner core growth, thus $^{186}$Os/$^{188}$Os in the outer core has increased. If material exchange occurs at the core-mantle boundary, mantle plumes of this deep origin (from D'' layer) could potentially be identified using W- and Os-isotopic tracers (Brandon et al., 1999; Brandon et al., 2003).

Noble gases (particularly helium) have long been used to distinguish plume from upper mantle sources (Graham, 2002). Depleted upper mantle has $^{3}$He/$^{4}$He ratios of 8-9 Ra (Ra = atmospheric ratio). Mantle plumes with elevated $^{3}$He/$^{4}$He are considered to come from the less-evolved mantle domain, presumably the deep mantle (e.g., Graham, 2002; Kurz et al., 2004). Some hotspots show lower $^{3}$He/$^{4}$He than MORB value, which is interpreted to reflect melting from recycled material like old oceanic crust and sediment that is incorporated into plumes through slab penetration to the deep mantle (e.g., Hanyu and Kaneoka, 1997). One of the major questions in mantle geochemistry is, where are the reservoirs of primitive (less-evolved) mantle and down-going recycled material? Are they layered above the D" boundary layer or mixed in the D'' layer (Ito and Mahoney, 2006; Xie and Tackley, 2004)? If we can identify a plume of the deep origin (by W and Os, for instance), noble gases coupled with radiogenic isotopes may provide answers to these questions.

In addition to noble gases, other volatiles are important tracers of mantle sources. For example, water and carbon dioxide may be relatively enriched or depleted in the mantle (upper, lower, D") through variable melting histories and slab recycling. Recent studies suggest that mantle minerals can contain more water than previously thought (Kohlstedt et al., 1996; Murakami et al., 2002). In particular, mantle rocks in the transition zone can be a sink for water (as well as elements that are partitioned with water) derived from subducted slabs (Bercovici and Karato, 2003). Plumes of upper-mantle or transition zone origin (identified by seismic tomography, for example), may also be characterized by higher concentrations of volatiles in melt inclusions in phenocrysts in addition to diagnostic O-isotopes and noble gases.

**7. Geochemical Assessment of Hotspot-Ridge Interaction**

When hotspots (plumes) are located near mid-ocean ridges, there are significant geochemical and geophysical interactions. These are important to evaluate in terms of the geodynamic goals of drilling along the targeted hotspot chains – namely, assessing hotspot motion, estimating the depth, temperature, and magma flux of plumes, and documenting the geochemical variability of mantle sources. Mid-ocean ridge basalts are distinguished from deeper mantle sources for plumes by depleted incompatible element concentrations, lower $^{87}$Sr/$^{86}$Sr and Pb-isotopic ratios, higher $^{143}$Nd/$^{144}$Nd and $^{176}$Hf/$^{177}$Hf ratios, and a narrower range of $^{3}$He/$^{4}$He ratios.

Lateral plume flow may feed seamount construction over a region between the hotspot and a nearby spreading ridge. In the case of the Galapagos hotspot, seamounts are distributed over ~200km from the plume stem beneath Fernandina Island to the Galapagos Spreading Center (Figure 13). In the Easter-Salas y Gomez chain, seamounts have been built by plume flow toward the East pacific Rise over a distance of ~450km. If undetected in any of the older parts of chains considered for drilling, seamounts formed by lateral plume flow could result in a 2-4° mis-location of the hotspot position. Plumes influence the morphology and geochemistry of adjacent ridges over much greater distances through sub-lithospheric flow (Schilling, 1991; Mittelstaedt and Ito, 2005), although the geometry of the transport (narrow pipelines vs broad gravity currents) is debated (Harpp and White, 2001; Harpp and Geist, 2002).

Fortunately, there are several geochemical and geophysical indicators of plume-ridge interaction along a hotspot chain. Radiogenic isotopic compositions of erupted material, specifically Sr, Nd, Pb, and Hf-isotopic ratios, are arguably the most useful geochemical measurements. These ratios remain unaffected by melting and crystallization processes, which allows for characterization of the mantle source or sources, critical information in deciphering relative contributions of plume *versus* upper mantle reservoirs. Nd, Hf, and Pb-isotopic compositions are only slightly affected by hydrothermal alteration and seafloor weathering, owing to the low concentrations of those elements in seawater; Sr-isotopic compositions are more strongly affected. The Os-isotopic system may also be especially useful in distinguishing plume from upper mantle sources, but analyses are difficult and data remain sparse (e.g., Hauri et al., 1996). Furthermore, Os is likely to be most useful when applied to xenoliths, often rare in shield stage lava flows (e.g., Meisel et al., 2001).

Incompatible trace elements should also be measured in concert with radiogenic isotope ratios. Even though trace element concentrations can be affected by melting and fractionation, ratios of incompatible trace elements often correlate with radiogenic isotope ratios, and can be used as supporting data for source characterization. Ratios of $^{3}He/^{4}He$ and other noble gases such as Ne have great potential for identifying primordial mantle material. Reliable He isotopic measurements require abundant, unaltered olivine in general, sometimes difficult to find although not usually a major challenge in submarine basalts.

Geophysically, several observations are important for identifying likely plume-ridge interaction. Broad, diffuse distributions of seamounts and oblique, volcanic lineaments between the spreading ridges and hotspots are common indicators of transport of plume material to the ridges (e.g., Galapagos and Easter). Asymmetric spreading and transform faults along ridges near the hotspot centers may also reflect increased heat supply from the plumes. Seamounts formed at ridges are isostatically compensated, whereas those formed off-ridge show isostatic anomalies (Watts, 1982; Small, 1995; Royer and Schlich, 1988).

The Emperor seamounts portion of the Hawaiian hotspot chain illustrates an example of the use of geochemical tracers to assess hotspot-ridge interaction. At about 81 Ma, the Hawaiian plume was near the Kula-Pacific speading ridge, and the lavas from that age until 61 Ma

(Suiko seamount, ~1000 km south) are more depleted geochemically than their modern counterparts. This has been interpreted in two ways. First, it has been proposed that when the ridge was close to the plume, contamination of the plume by the upper mantle was stronger (Keller et al., 2004). A second hypothesis is that when a plume rises near a ridge, the lithospheric "lid" is thinner, permitting shallower and more extensive melting of a depleted component intrinsic to the plume (Regelous, 2003). Thus, a significant fraction of the depleted component may be more directly attributable to thin lithosphere than to ridge interaction. Detailed knowledge of the multiple components carried in the plume is required to evaluate which of these is more significant.

Of the four hotspot chains that are targeted for drilling, the Louisville ridge has formed well away from the influence of the closest ridge, the East Pacific Rise, and is not expected to be significantly affected by hotspot-ridge interaction. This is not the case for the Walvis, Chagos-Maldive, and Ninetyeast ridges, all of which have formed in part when hotspots were at or near spreading ridges. For these three chains, detailed tectonic reconstructions are required to determine the plume-ridge separation at the time specific seamounts were constructed. Interpretations of plume and ridge contributions will have to be based on geophysical evaluation of seamount morphology and isostatic compensation, multiple geochemical tracers of the core samples, and complete understanding of Tristan, Reunion and Kerguelen plume compositions.

**8. Mantle potential temperatures**

According to one school of thought, high potential temperature is the defining characteristic of a mantle plume. As indicated by the term "hotspot", the sources of oceanic islands and other such features are parts of the mantle that melt preferentially because they are hotter than ambient mantle. Another school disputes this interpretation and attributes high magma flux to a more "fertile" (easily fusible) source, or to the presence of water or other volatiles, or to tectonic factors. The debate started over a decade ago and continues.

The "hot" hotspot school generally envisages a plume as a roughly cylinder-shaped region of mantle that rises from a site deep in the mantle, well beneath moving plates. The plume rises from a boundary layer, perhaps the core-mantle boundary, perhaps at the base of the upper mantle, and it ascends because its high temperature gives it buoyancy. From this viewpoint, plumes are seen as a mode of mantle convection that operates largely independently from plate tectonics. From the other viewpoint, hotspots are commonly seen as an integral part of the plate tectonic process and unrelated to deep mantle processes. Resolution of the question therefore has profound implications for our understanding of mantle dynamics, including the composition and heterogeneity of the mantle, its heat balance, and the way it melts. Taking the argument one step further, the large igneous provinces that formed episodically through geological history are, in the view of the first school, the product of melting of a vast hot mantle plume head. The other school prefers to relate their formation to the distribution and dynamics of the lithospheric plates.

One of the keys to resolving the argument is the determination of the temperatures of magmas generated from hotspots. To obtain this information is not a simple matter of measuring eruption temperatures because most magmas have undergone some degree of

fractional crystallization and their temperatures are lower than those of primary melts of the mantle source. To determine the temperature of the source requires that the temperature at the site of melting is determined. In most cases the source is thermally zoned. In the ideal case, the temperatures of formation of a series of primary magmas would be established so as to characterize the complete temperature variation of the source. Petrological/geochemical methods provide little information, however, about median temperatures in the source because of the camouflaging effects of fractional crystallization. However, the maximum temperatures in the source can be established.

The approach is to use composition of the most magnesian olivine analyzed in a suite of samples. There is a direct relation between the Mg/Fe of olivine and that of the liquid from which the olivine crystallized. The FeO contents of basaltic to picritic liquids vary little during fractional crystallization and the FeO contents of probable parental liquids are readily estimated. From this we can calculate the MgO contents of the liquids, a parameter that is directly related to the temperature of the magma. The final step is to translate the temperature of crystallization at low pressure prior to or during eruption of the magma to that at the site of melting deeper in the mantle. The source temperature is commonly expressed as "potential temperature", which is the temperature at the site of melting extrapolated along a solid adiabat to the surface.

Application of this approach to mafic and ultramafic magmas worldwide yields a wide range of temperatures: for normal MORB the maximum eruption temperature is about 1200°C and the potential temperature is about 1350°C; for lavas from Hawaii, the hottest modern plume, the figures are 1400°C and >1800°C; and for Archean komatiites they are 1650°C and >2000°C. Members of the opposing school dispute these figures, arguing that by selection of another set of assumptions and different choices of partition coefficients, the calculated temperatures are far lower. In particular, it has been argued that by assuming moderate to high water contents in the source, the eruption temperatures of Hawaiian basalts, and even those of komatiites, are little higher than those of MORB.

To obtain information about the average temperature, and the distribution of temperatures in the source of magmas at hotspots, indirect methods can be used. In well-dated, well-studied volcanoes, magma fluxes can be estimated by calculating the volume of emplaced magma as a function of time, or by using geophysical and tectonic data to determine the extent and nature of deformation of the lithosphere above a hotspot. Seismic tomography in some cases can be used to image the geometry and physical characteristics of the region in which melting takes place. In theory it is possible to relate seismic properties to the temperature of the source; in practice this is not straightforward because it is very difficult to take into account the influence of composition, mineralogy and physical state of the source.

A particularly important issue is the composition of the source. Up until now most attempts to extract information about source temperatures have been based implicitly or explicitly on the assumption that the source was broadly peridotitic. Various lines of evidence have shown that the sources of many mafic-ultramafic magmas contain a significant proportion of recycled oceanic crust. The presence of this material must be taken into account when calculating magma fluxes and temperatures. Other elements that require attention are the oxygen fugacity

in the source, which affects melting relations and Mg-Fe partitioning, and of course the nature and amount of volatiles.

Determination of the potential temperature of the source should be an integral part of the petrological-petrogenetic study of any volcanic series. Core from virtually all ocean drilling sites will contain olivine-phyric basalts and the study of these basalts, olivine compositions, and the composition of melt inclusions in olivine phenocrysts will yield information about source temperatures. In most cases, however, the majority of recovered basalts represent evolved magmas. To address directly the issue of source temperature requires that the most magnesian lavas be targeted; yet we have no reliable means of predicting where in a volcanic series such magmas will be found. There is some tendency for them to occur deep in the stratigraphic pile. However, in chains of complex volcanoes formed on a moving plate such as at Hawaii, the stratigraphy is complicated and prediction is hazardous. Picrites are where you find them, but when they are found they provide valuable information.

## II. A GLOBAL DRILLING PLAN

We propose a global ocean drilling strategy that extends the ODP Leg 197 drilling, logging and post-cruise science plan as a model to include several additional (3-4) hotspot tracks formed during the same interval (80-49 Ma). These additional drilling targets will be: **(i)** a second major Pacific plate hotspot track (Louisville ridge), **(ii)** two north-south oriented Indian Ocean hotspot tracks (Chagos-Maldives and Ninetyeast ridges), and **(iii)** an Atlantic basin hotspot track tied to the African plate (Walvis ridge). Drilling a minimum of 3 sites along each hotspot track, shipboard measurements and post-cruise studies will provide:

**1.** Paleolatitudes at comparable ages to Emperor seamount sites (80, 61, 56 and 49 Ma) for a global test of predicted hotspot motions and whole Earth motion with respect to the spin axis.
**2.** Radiometric ages to construct the necessary framework for hotspot track comparisons, plate reconstructions, and volcano evolution.
**3.** Synthetic plate polar wander paths assembled by combining data from continental portions of plates with the paleolatitude measurements.
**4.** Geochemical data to assess hotspot-ridge and plume-lithosphere interactions, plume source, temperature, depth and along-track evolution.

The essential geodynamic experiment has two parts: **(i)** hotspot motion, and **(ii)** plume composition and evolution. The first part uses paleomagnetic estimates of hotspot paleolatitudes in combination with radiometric ages and hotspot chain geometry to test the predictions of mantle flow models of hotspot motion. The most recent model results from Steinberger and Antretter (2006) are illustrated in Figure 14 for seven major hotspots. The observed ~15° southward motion of Hawaii between 80 and 49 Ma is compatible with this model. Other hotspots are predicted to have moved (latitudinally) very little (Louisville, Reunion, Tristan) or northward a small amount (Kerguelen) in this period. Hence, if hotspot motion is purely a result of plume advection in mantle flow, paleolatitudes determined from the Louisville, Reunion, Kerguelen and Tristan hotspot tracks should be within a few degrees of present latitudes. If, however, changes in the distribution of gravitational heterogeneities

caused by plate motions and convection in the mantle are significant enough to cause whole Earth motion (Goldreich and Toomre, 1969) we should detect a northward motion (4-5° since 50 Ma) for the Tristan hotspot track. The two processes combine to predict northward motion for the Kerguelen hotspot (~6° during 80-50 Ma) and slow southward motion of the Louisville hotspot (5-6° since 60 Ma). Reunion hotspot should have remained close to its present latitude throughout its 65 Ma history.

Many of these predicted motions are at the lower limit of resolution, given the practical constraints of ocean drilling. However, the consistency in direction and magnitude of paleolatitudes measured from these globally distributed, major hotspot tracks will provide a strong test of the predictions of both mantle flow and whole earth motion models. ODP Leg 197 has shown the potential for a major improvement in the mantle-based reference frame to include hotspot motion, but confirmation within and outside the Pacific basin is required.

The second part uses the deep sampling of shield-building lava flows at several locations along these major hotspot tracks, together with dredge samples from a much larger number of locations, to determine (through a combination of geochemical methods) the origin, composition and variability of plume, upper mantle and lithospheric contributions to hotspot melting. Within the hotspot tracks considered are examples of hotspots beginning near a spreading ridge and crossing the ridge, but becoming intra-plate with time (Hawaii, Reunion, Kerguelen and Tristan), and a hotspot that has been intra-plate throughout (Louisville). Drilling into the main shield-building stage at Louisville volcanic systems will also examine the surprising uniformity of dredge samples from this chain and test the proposed link with the Ontong Java plateau.

After reviewing existing drilling proposals in the IODP science advisory system, we believe that all elements of this global strategy are potentially identified in the targeted hotspot tracks. Specific tests and outcomes are discussed in the next section.

## III. RECOMMENDATIONS

Our prioritized order of drilling programs is:

**1. The Louisville Ridge program (Proposal 636-Full2)** is a Pacific plate complement to the Emperor Seamounts program (ODP Leg 197 and DSDP Site 433). It should focus on a minimum of 3 sites to achieve more than 250 m penetration and recovery of core at each site for the paleolatitude test of Louisville hotspot motion. The outcome will determine the latitudinal motion of the hotspot during the period 80-49 Ma to reach these alternate conclusions: (1) increasing southward motion with age comparable to Hawaii (up to ~15°), indicating a common motion of the mantle underlying the Pacific plate with respect to the spin axis (whole Earth polar motion), or (2) no discernable motion, supporting mantle flow models. Geochemical data from shield-stage lavas will (a) test the hypothesized connection between Louisville Ridge and the Ontong Java Plateau, (b) document geochemical variability of hotspot products along this chain where the hotspot-lithosphere age difference is ~constant, in contrast to Hawaii, Reunion, Kerguelen and Tristan hotspot tracks, and (c) describe the magma flux behavior of the plume source over 80 m.y. This program, pending

full assessment of post-site-survey data and post-cruise results, could move quickly to scheduling.

**2. The Chagos-Maldives Ridge and Ninetyeast Ridge program (proposal 620-Full3)** relies heavily on re-occupation of previously drilled DSDP and ODP sites (214, 216, 713, 715, 756 and 758), where shallow penetration of basement established the age and paleomagnetic potential for the Kerguelen and Reunion hotspot motion tests. Site survey data for the Ninetyeast Ridge sites will be acquired summer 2007 (*R/V Revelle*). We have concerns for the Ninetyeast Ridge sites about post-volcanic faulting or tilting, and possible reversals in the northward aging of volcanic centers due to ridge jumps must be carefully evaluated. Although the Reunion hotspot track terminates with the Deccan flood basalts (65 Ma) and does not offer a complete comparison with the Emperor seamount experiment, extending drilling at sites 713 and 715 to 250 m+ depths could produce two high-resolution paleolatitudes, for comparison with the well-determined Deccan paleolatitude. Mantle flow models predict no discernable latitudinal motion for Reunion (65-49 Ma) but small northward motion (~4°) for Kerguelen (80-49 Ma), while whole Earth motion models predict ~3° northward motion for Reunion between 65 and 45 Ma, and ~4° northward motion for Kerguelen between 65 and 45 Ma.

**3. The Tristan-Walvis Ridge program (669-Pre)** focuses on the most complete and continuous, long-lived hotspot track, linking a large igneous province erupted during continental breakup with an age-progressive volcanic chain, changing from ridge-centered to off-ridge hotspot setting. In addition, this hotspot track forms the central mantle-based reference for all global plate reconstructions tied to the African plate. It is also, then, directly tied to the synthetic continental apparent polar wander path. We give this program lower priority only because of lack of site survey data. Re-occupation of DSDP Site 525 (~80 Ma) to achieve more than 250 m penetration for paleolatitude is the most immediately achievable goal. Younger sites, comparable to Emperor seamount paleolatitude sites, are desirable but cannot be selected from existing data. We note that a German expedition is scheduled for mapping and dredging the southwestern portion of the province in 2008. Mantle flow models predict no discernable latitudinal motion for 80-49 Ma, while whole Earth motion models predict ~7-8° southward motion for the same period. A site on the Walvis Ridge near the continental margin (~110 Ma) is attractive because it would test the maximum predicted whole Earth polar motion (~10-15° southward, 110 to 50 Ma) derived from continental paleomagnetic studies, and provide information about the combined geometry of plume and LIP soon after continental breakup. Again, site survey data are needed to optimize the location of this site.

We have several general recommendations about site selection and drilling plans for any of these programs:

(1) Holes should be sited near seamount summits, rather than steep flanks to avoid tectonic disturbances and to most optimally intersect the waning phase of the shield stage activity. The ideal drilling site is a section of lava flows accumulated from a time series of separate eruptions that have traveled a significant distance from source. Evidence of time (to fully sample paleo-secular variation) is soil interbeds, a preponderance of lava

flows over volcaniclastic units, compositional changes, and variation in paleoinclination – all of which should be monitored during drilling operations.

(2) Drilling penetration should be sufficient to recover 20 to 30 lava units in order to provide a nominal 4-5° $\alpha_{95}$ on paleolatitude estimates (Figure 15). From previous experience, this is requires at least 250 to 350m of drilling in basaltic basement. Real-time monitoring of onboard paleomagnetic data, geochemical data, and physical volcanology is required to determine the termination depth at each site. This depth of penetration will require multiple bit changes and re-entry capability.

(3) Pre-cruise planning of each drilling environment must evaluate guidebase and casing versus free-fall funnel re-entry strategies.

(4) Extensive dredging during site surveying will be crucial to provide a detailed geochronology and geochemistry framework in which to interpret the drilling results.

## IV. REFERENCES


Acton, G. D., 1999. Apparent polar wander of India since the Cretaceous with implications for regional tectonics and true polar wander, In, The Indian subcontinent and Gondwana, Mem. **44**, T. Radhakrishna and J. D. A. Piper, eds., *Geol. Soc. India*, Bangalore, 129-175.

Anson, G. L., and K.P. Kodama, 1987. Compaction-induced inclination shallowing of the post-depositional remanent magnetization in a synthetic sediment, *Geophys. J. R. Astr. Soc.,* **88**, 673-692.

Antretter, M., Steinberger, B., Heider, F. and So el, H., 2002. Paleolatitudes of the Kerguelen hotspot: New paleomagnetic results and dynamic modeling, *Earth Planet. Sci. Lett.,* 203, 635-650, doi:10.1016/S0012-821X(02)00841-5

Antretter, M., Riisager, P., Hall, S., Zhao, X., and Steinberger, B., 2004. Modeled paleolatitudes for the Louisville hotspot and the Ontong Java Plateau. In, Origin and Evolution of the Ontong Java Plateau, *Geol. Soc. (London) Spec. Publ.,* 229, pp. 21-30, G. Fitton, J. Mahoney, P. Wallace, and A. Saunders (eds), The Geological Society, London.

Beaman, M., W. W. Sager, G. D. Acton, L. Lanci, and J. Parés, 2007. Improved Late Cretaceous and early Cenozoic paleomagnetic apparent polar wander path for the Pacific plate, *Earth Planet. Sci. Lett.*, submitted.

Bercovici, D., and S. Karato, 2003. Whole-mantle convection and the transition-zone water filter. *Nature*, **425**, 39-44.

Besse, J., and V. Courtillot, 1991. Revised and synthetic polar wander paths of the African, Eurasian, North American, and Indian plates and true polar wander since 200 Ma, *J. Geophys. Res*., **96**, 4,029-4,050.

Besse, J. and V. Courtillot, V., 2002. Apparent and true polar wander and the geometry of the geomagnetic field over the last 200 Myr, *J. Geophys. Res.,* **107**, 2300, doi: 10.1029/2000JB000050.

Brandon, A.D., M.D. Norman, R.J. Walker, and J.W. Morgan, 1999. $^{186}Os$-$^{187}Os$ systematics of Hawaiian picrites. *Earth Planet. Sci. Lett.*, *174*, 25-42.

Brandon, A.D., R.J. Walker, I.S. Puchtel, H. Becker, M. Humayun, and S. Revillon, 2003. $^{186}Os$-$^{187}Os$ systematics of Gorgona Island komatiites: implications for early growth of the inner core. *Earth Planet. Sci. Lett.*, *206*, 411-426.

Bryce, J.G., D.J. DePaolo, and J.C. Lassiter, 2005. Geochemical structure of the Hawaiian plume: Sr, Nd, and Os isotopes in the 2.8 km HSDP-2 section of Mauna Kea volcano. *Geochem. Geophys. Geosyst.*, *6*, doi: 10.1029/2004GC000809.

Cande, S.C. and Kent, D.V., 1995. Revised calibration of the geomagnetic polarity time scale for the Late Cretaceous and Cenozoic. *J. Geophys. Res*., 100: 6093-6095.

Cande, S.C., Raymond, C.A., Stock, J. and Haxby, W.F., 1995. Geophysics of the Pitman Fracture Zone and Pacific-Antarctic plate motions during the Cenozoic. *Science*, 270: 947-953.

Chave, A.D., 1984. Lower Paleocene-Upper Cretaceous magnetostratigraphy, sites 525-527,528, and 529, Deep Sea Drilling Project Leg 74. *Init. Repts DSDP*, 74: 525-531.

Cheng, Q., K.-H. Park, et al., 1987. Isotopic evidence for a hotspot origin of the Louisville seamount chain. *Seamounts, Islands and Atolls.* B. H. Keating, P. Fryer, R. Batiza and G. W. Boehlert. Washington, D.C., American Geophysical Union Monograph. **43:** 283-296.

Clague, D.A. and Dalrymple, G.B., 1987. The Hawaiian-Emperor volcanic chain. In, Decker, R.W., Wright, T.L. and Stauffer, P.H. (eds), *Volcanism in Hawaii* (US Government Printing Office), pp. 5-54.

Cottrell, R. D., and J. A. Tarduno, J. A., 2003, A Late Cretaceous pole for the Pacific plate: Implications for apparent and true polar wander and the drift of hotspots, *Tectonophysics*, **362**, 321-333, 2003.

Cox, A., and R. G. Gordon, 1984. Paleolatitudes determined from paleomagnetic data from vertical cores, *Rev. Geophys. Space Phys*., **22**, 47-72.

Dalrymple, G.B. and Clague, D.A., 1976. Age of the Hawaiian-Emperor bend. *Earth Planet. Sci. Lett.* 31, 313-329.

Dalrymple, G.B., Clague, D.A. and Lanphere, M.A., 1977. Revised age for Midway volcano, Hawaiian volcanic chain. *Earth Planet. Sci. Lett.* 37, 107-116.

De Paolo, D.J., J.G. Bryce, A. Dodson, D.L. Shuster, and B.M. Kennedy, 2001. Isotopic evolution of Mauna Loa and the chemical structure of the Hawaiian plume. *Geochem. Geophys. Geosyst.*, *2*, doi:10.1029/2000GC000139.

Doubrovine, P.V. and Tarduno, J.A., 2004. The Late Cretaceous paleolatitude of the Hawaiian hot spot: new paleomagnetic data from Detroit Seamount. *Geochem. Geophys. Geosys.*, 5:Q11L04. doi:10.1029/2004GC000745.

Duncan, R.A., 1981. Hotspots in the southern oceans—an absolute frame of reference for motion of the Gondwana continents. *Tectonophysics*, **74**:29-42.

Duncan, R.A. and Clague, D.A., 1985. Pacific plate motion recorded by linear volcanic chains. In: *The ocean basins and margins. A.E.A. Nairn, F.L. Stehli and S. Uyeda. New York, Plenum Press. 7A: The Pacific ocean(Issue), 89-121*.

Duncan, R.A. and Keller, R.A., 2004. Radiometric ages for basement rocks from the Emperor Seamounts, ODP Leg 197. *Geochem. Geophys. Geosys.* 5, Q08L03, doi: 10.1029/2004GC000704.

Duncan, R.A. and I. McDougall, 1976. Linear volcanism in French Polynesia. *J. Volcanol. Geotherm Res*., **1**:197-227.

Eisele, J., W. Abouchami, S.J.G. Galer, and A.W. Hofmann, 2003. The 320 kyr Pb isotope evolution of Mauna Kea lavas recorded in the HSDP-s drill core. *Geochem. Geophys. Geosyst.*, *4*, doi:10.1029/2002GC000339.

Frey, F.A., Huang, S., Blichert-Toft, J. Regelous, M., and Boyet, M., 2005. Origin of depleted components in basalt related to the Hawaiian hot spot: evidence from isotopic and incompatible element ratios. *Geochem. Geophys. Geosys.* 6(2):Q02L07. doi:10.1029/2004GC000757.

Goldreich, P. and Toomre, A., 1969. Some remarks on polar wandering. *J. Geophys. Res.*, 74: 2555-2567.

Gordon, R.G. and Cox, A., 1980. Calculating palaeomagnetic poles for oceanic plates. *Geophys. J. R. Astr. Soc.*, 63: 619-640.

Graham, D. W., 2002. Noble gas isotope geochemistry of mid-ocean ridge and ocean island basalts: Characterization of mantle source reservoirs. *Noble Gases in Geochemistry and Cosmochemistry.* D. Porcelli, C. J. Ballentine and R. Wieler. Washington, D.C., Mineralogical Society of America**:** 247-318.

Hanyu, T., and I. Kaneoka, 1997. The uniform and low $^{3}He/^{4}He$ ratios of HIMU basalts as evidence for their origin as recycled materials. *Nature*, *390*, 273-276.

Harpp, K. S. and D. J. Geist, 2002. The Wolf-Darwin Lineament and plume-ridge interaction in the Northern Galapagos. *Geochem. Geophys. Geosys.* **3**: doi:10.1029/2002GC000370.

Harpp, K. S. and W. M. White, 2001. Tracing a mantle plume: Isotopic and trace element variations of Galapagos seamounts. *Geochem. Geophys. Geosys.* **2**: 200GC00137.

Hauri, E. H., J. C. Lassiter, et al., 1996. Osmium isotope systematics of drilled lavas from Mauna Loa, Hawaii. *J. Geophys. Res.* **101**: 11793-11806.

Hawkins, J. W., P. F. Lonsdale, et al., 1987. Petrologic evolution of the Louisville seamount chain. *Seamounts, Islands and Atolls.* B. H. Keating, P. Fryer and R. Batiza. Washington, D.C., American Geophysical Union Monograph. **43:** 235-254.

Hodych, J. P., S. Bijaksana, and R. Pätzold, 1999. Using magnetic anisotropy to correct for paleomagnetic inclination shallowing in some magnetite-bearing deep-sea turbidites and limestones, *Tectonophysics,* **307**, 191-205.

Inokuchi, H. and Heider, F. 1992. Magnetistratigraphy of sediments from Sites 748 and 750, Leg 120. In, Wise, S.W., Jr., Schlich, R. et al. (eds), *Proc. ODP, Sci. Results*, 120: 247-252.

Ito, G., and J.J. Mahoney, 2006. Melting a high $^{3}He/^{4}He$ source in a heterogeneous mantle. *Geochem. Geophys. Geosyst.*, *7*, doi:10.1029/2005GC001158.

Keller, R. A., D. W. Graham, et al., 2004. Cretaceous-to-recent record of elevated $^{3}He/^{4}He$ along the Hawaiian-Emperor volcanic chain. *Geochem. Geophys. Geosys.* **5** (Q12L05): doi:10.1029/2004GC000739.

Kirkwood, B. H., J.-Y. Royer, T. C. Chang, and R. G. Gordon, 1999. Statistical tools for estimating and combining finite rotations and their uncertainties," *Geophys. J. Int.,* 137: 408-428.

Kleine, T., C. Munker, K. Mezger, and H. Palme, 2002. Rapid accretion and early core formation on asteroids and the terrestrial planets from Hf-W chronometry. *Nature*, *418*, 952-955.

Klootwijk, C.T., Gee, J.S., Peirce, J.W. and Smith, G.M., 1991. Constraints on the India-Asia convergence: Paleomagnetic results from Ninetyeast Ridge. *Proc. ODP, Sci. Results*, 121: 777-882.

Kohlstedt, D., H. Keppler, and D. Rubie, 1996. Solubility of water in the alpha, beta and gamma phases of $(Mg,Fe)SiO_4$. *Contrib. Mineral. Petrol.*, *123*, 345-357.

Kono, M., 1980. Paleomagnetism of DSDP Leg 55 basalts and implications for the tectonics of the Pacific plate. In, Jackson, E.D., Koizumi, I. et al., *Init. Repts. DSDP,* 55: Washington (U.S. Govt Printing Office), 737-752.

Koppers, A.A.P., Staudigel, H. and Wijbrans, J.R., 2000. Dating crystalline groundmass separates of altered Cretaceous seamount basalts by the Ar-40/Ar-39 incremental heating technique. *Chem. Geol.* 166(1-2), 139-158.

Koppers, A.A.P., H. Staudigel, M. S. Pringle, J. R. Wijbrans, 2003. Short-lived and discontinuous intraplate volcanism in the South Pacific: Hot spots or extensional volcanism?, *Geochem. Geophys. Geosyst.*, 4 (10), 1089, doi:10.1029/2003GC000533.

Koppers, A.A.P., Duncan, R.A. and Steinberger, B., 2004. Implications of a non-linear $^{40}Ar/^{39}Ar$ age progression along the Louisville seamount trail for models of fixed and moving hotspots. *Geochem. Geophys. Geosys.* 5(6), doi:10.1029/2003GC000671.

Kurz, M.D., J. Curtice, and D.E. Lott III, 2004. Rapid helium isotopic variability in Mauna Kea shield lavas from the Hawaiian Scientific Drilling Project. *Geochem. Geophys. Geosyst.*, *5*, doi:10.1029/2002GC000439.

Larson, R. L., and Sager, W. W., 1992. Skewness of magnetic anomalies M0 to M29 in the northwestern Pacific, *Proc. ODP, Sci. Res.*, **129**, 471-481.

Lassiter, J.C., and E.H. Hauri, 1998. Osmium-isotope variations in Hawaiian lavas: evidence for recycled oceanic lithosphere in the Hawaiian plume. *Earth Planet. Sci. Lett.*, *164*, 483-496.

Lonsdale, P., 1988. Geography and history of the Louisville Hotspot Chain in the southwest Pacific. *J. Geophys. Res.* **93** (B4): 3078-3104.

Mayer, L. and Tarduno, J.A., 1993. Paleomagnetic investigation of the igneous sequence, Site 807, Ontong Java Plateau, and a discussion of Pacific true polar wander. In, Berger, W.H., Kroenke, L.W., Mayer, L.A. et al. (eds), *Proc. ODP, Sci. Results,* 130: 51-59.

McElhinny, M.W., P. L. McFadden, and R. T. Merrill, 1996. The time-averaged paleomagnetic field 0–5 Ma, *J. Geophys. Res.*, **101**: 25,007–25,027.

Meisel, T., R. J. Walker, et al., 2001. Osmium isotopic compositions of mantle xenoliths: A global perspective. *Geochim. Cosmochim. Acta* **65**: 1311-1323.

Merrill, R. T., M. W. McElhinny, and P. L. McFadden, P. L., 1996. *The Magnetic Field of the Earth*, New York, Academic Press, 531 pp.

Merrill, R. T., and P. L. McFadden, 2003. The geomagnetic axial dipole field assumption, *Phys. Earth Planet. Int.*, **139**, 171-185, 2003.

Mittelstaedt, E. and G. Ito, 2005. Plume-ridge interaction, lithospheric stresses, and the origin of near-ridge volcanic lineaments. *Geochem. Geophys. Geosys.* **6** (6): Q06002, doi:10.1029/2004GC000860.

Morgan, W.J., 1972a. Deep mantle convection plumes and plate motions. *Amer. Assoc. Petrol. Geol. Bull.* 56, 42-43.

Morgan, W.J., 1972b. Plate motions and deep mantle convection. *Geol. Soc. Amer. Mem.* 132 (Hess Volume), 7-122.

Morgan, W.J., 1981. Hotspot tracks and the opening of the Atlantic and Indian Oceans. In: C. Emiliani (Editor). Wiley-Interscience, New York, pp. 443-487.

Muller, R. D., W. R. Roest, J.-Y. Royer, L. M. Gahagan, and J. G. Sclater, 1997. Digital isochrons of the world's ocean floor, *J. Geophys. Res.*, 102, 3211-3214.

Murakami, M., K. Hirose, H. Yurimoto, S. Nakashima, and N. Takafuji, 2002. Water in earth's lower mantle. *Science*, *295*, 1885-1887.

Nakanishi, M. and Gee, J 1995. Paleomagnetic investigation of volcanic rocks: Paleolatitudes of the northwestern Pacific guyots. *Proc. ODP, Sci. Results*, 144, doi: 10.2973/odp.proc.sr.144.022.1995.

O'Connor, J.M. and Le Roex, A.P., 1992. South Atlantic hot spot-plume systems: 1. Distribution of volcanism in time and space. *Earth Planet. Sci. Lett.*, 113: 343-364.

O'Neill, C., Muller, D. and Steinberger, B., 2005. On the uncertainties in hotspot reconstructions, and the significance of moving hotspot reference frames. *Geochem. Geophys. Geosyst.*, 6, Q04003, doi:10.1029/2004GC000784.

Petronotis, K. E., and R. G. Gordon, R. G., 1999. A Maastrichtian paleomagnetic pole for the Pacific plate from a skewness analysis of marine magnetic anomaly 32, *Geophys. J. Int.*, **139**, 227-247.

Petronotis, K. E., R.G. Gordon, and G.D. Acton, 1992. Determining paleomagnetic poles and anomalous skewness from marine magnetic anomaly skewness data from a single plate, *Geophys. J. Int.,* **109**, 209-224.

Prévot, M., E. Mattern, P. Camps, and M. Dagnieres, 2000, Evidence for a 20° tilting of the Earth's rotation axis 110 million years ago, *Earth Planet. Sci. Lett*., **179**, 517-528, 2000.

Regelous, M., 2003. Geochemistry of lavas from the Emperor Seamounts, and the geochemical evolution of Hawaiian magmatism from 85 to 42 Ma. *J. Petrol.* **44**(1): 113-140.

Ribe, N.M., and U.R. Christensen, 1999. The dynamical origin of Hawaiian volcanism, *Earth Planet. Sci. Lett.*, *171*, 517-531.

Richards, M.L., V. Vacquier, and G. D. Van Voorhis, 1967. Calculations of the magnetization of uplifts from combining topographic and magnetic surveys, *Geophysics*. **32**: 678-707.

Riisager, P., Hall, S., Antretter, M. and Zhao, X., 2003. Paleomagnetic paleolatitude of Early Cretaceous Ontong Java basalts: implications for Pacific apparent and true polar wander. *Earth Planet. Sci. Lett.*, 208: 235-252.

Royer, J. Y. and R. Schlich, 1988. Southeast Indian Ridge between the Rodriguez Triple Junction and the Amsterdam and Saint Paul Islands: Detailed kinematics for the past 20 m.y. *J. Geophys. Res.* **93**: 13524-13550.

Sager, W. W., 2006. Cretaceous paleomagnetic apparent polar wander path for the Pacific plate calculated from Deep Sea Drilling Project and Ocean Drilling Program basalt cores, *Phys. Earth Planet. Int.*, **156**, 329-349.

Sager, W. W., 2007. Divergence between paleomagnetic and hotspot model predicted polar wander for the Pacific plate with implications for hotspot fixity, in *Plates, Plumes, and Planetary Processes*, Spec. Paper ###, G. R. Foulger and D. M. Jurdy, eds., Geol. Soc. Amer., Boulder, CO.

Schettino, A., and C. R. Scotese, 2005. Apparent polar wander paths for the major continents (200 Ma to the present day): A palaeomagnetic reference frame for global plate tectonic reconstructions, *Geophys. J. Int*., **163**, 727-759.

Schilling, J.-G., 1991. Fluxes and excess temperatures of mantle plumes inferred from their interaction with migrating mid-ocean ridges. *Nature,* **352**: 397-403.

Schilling, J.-G., D. Fontignie, et al., 2003. Pb-Hf-Nd-Sr isotope variaitons along the Galapagos Spreading Center (101°-83°W): Constraints on the dispersal of the Galapagos mantle plume. *Geochem. Geophys. Geosys.* **4** (10): 8512, doi:10.1029/2002GC000495.

Schouten, H., and S. C. Cande, 1976. Palaeomagnetic poles from marine magnetic anomalies, *Geophys. J. R. Astr. Soc*., **44**, 567-575.

Sharp, W.D. and Clague, D.A., 2006. 50-Ma initiation of Hawaiian-Emperor bend records major change in Pacific plate motion. *Science* 313(5791), 1281-1284.

Small, C., 1995. Observations of ridge-hotspot interactions in the Southern Ocean. *J. Geophys. Res.* **100**(B9): 17931-17946.

Steinberger, B. and O'Connell, R. J., 1998. Advection of plumes in mantle flow: implications for hotspot motion, mantle viscosity and plume distribution, *Geophys. J. Int.*, 132, 412{434, doi:10.1046/j.1365-246x.1998.00447.x

Steinberger, B., 2000. Plumes in a convecting mantle: Models and observations for individual hotspots, *J. Geophys. Res.*, 105, 11,127-11,152, doi: 10.1029/1999JB900398

Steinberger, B., Sutherland, R., and O'Connell, R. J., 2004. Prediction of Emperor- Hawaii seamount locations from a revised model of global plate motion and mantle flow, *Nature,*

**430**, 167-173, doi:10.1038/nature02660.

Steinberger, B. and Antretter, M., 2006. Conduit diameter and buoyant rising speed of mantle plumes - implications for the motion of hotspots and shape of plume conduits, *Geochem. Geophys. Geosyst.*, 7, doi:10.1029/2006GC001049.

Stolper, E.M., D.J. De Paolo, and D.M. Thomas, 1996. Introduction to special section: Hawaii Scientific Drilling Project, *J. Geophys. Res.*, *101*, 11593-11598.

Tarduno, J. A., 1990. Absolute inclination values from deep sea sediments: A reexamination of the Cretaceous Pacific record, *Geophys. Res. Lett.,* **17**, 101-104.

Tarduno, J.A., and R. D. Cottrell, 1997. Paleomagnetic evidence for motion of the Hawaiian hotspot during formation of the Emperor Seamounts, *Earth Planet. Sci. Lett*., **153**, 171-180.

Tarduno, J.A., Duncan, R.A., Scholl, D.W., Cottrell, R.D., Steinberger, B., Thordarson, T., Kerr, B.C., Neal, C.R., Frey. F.A., Torii, M. and Carvallo, C., 2003. The Emperor Seamounts: Southward motion of the Hawaiian hotspot plume in Earth's mantle, *Science*, **301**, 1064-1069, doi: 10.1126/science.1086442.

Tarduno, J.A. and Sager, W.W., 1995. Polar standstill of the Mid-Cretaceous Pacific Plate and its geodynamic implications. *Science*, 269: 956-959.

Tauxe, L. and Kent, D.V., 2004. A simplified statistical model for the geomagnetic field and the detection of shallow bias in paleomagnetic inclinations: Was the ancient magnetic field dipolar? In: J.E.T. Channell, D.V. Kent, W. Lowrie and J. Meert (Editors), *Timescales of the Paleomagnetic Field*. AGU, Washington, D.C., pp. 101-115.

Torsvik, T. H., and R. Van der Voo, Refining Gondwana and Pangea palaeogeography: Estimates of Phanerozoic non-dipole (octupole) fields, *Geophys. J. Int.,* **151**, 771-794, 2002.

Van der Voo, R., 1993. Paleomagnetism of the Atlantic, Tethys and Iapetus Oceans. Cambridge University Press, Cambridge, 411 pp.

Van Fossen, M. C., and D. V. Kent, 1992. Paleomagnetism of 122 Ma plutons in New England and the Mid-Cretaceous paleomagnetic field in North America: True polar wander or large-scale differential mantle motion, *J. Geophys. Res*., **97**, 19651-19661.

Vasas, S. M., R. G. Gordon, and K. E. Petronotis, 1994. New paleomagnetic poles for the Pacific plate from analysis of the shapes of anomalies 33n and 33r, *EOS, Trans. AGU*, **75**, Fall Meeting Supplement, 203.

Watts, A.B. 1982. Seamounts and flexure of the lithosphere. *Nature*, 297: 182-183.

Watts, A.B., Weissel, J.K., Duncan, R.A. and Larson, R.L., 1988. Origin of the Louisville Ridge and its relationship to the Eltanin fracture zone system. *J. Geophys. Res. 93*, *3,051-3,077*.

Wessel, P., Y. Harada, and L. W. Kroenke, 2006. Toward a self-consistent, high-resolution absolute plate motion model for the Pacific, *Geochem. Geophys. Geosys*., **7**, Q03L12, doi: 10.1029/2005GC00100.

Xie, S., and P.J. Tackley, 2004. Evolution of helium and argon isotopes in a convecting mantle, *Phys. Earth Planet. Int.*, *146*, 417-439.

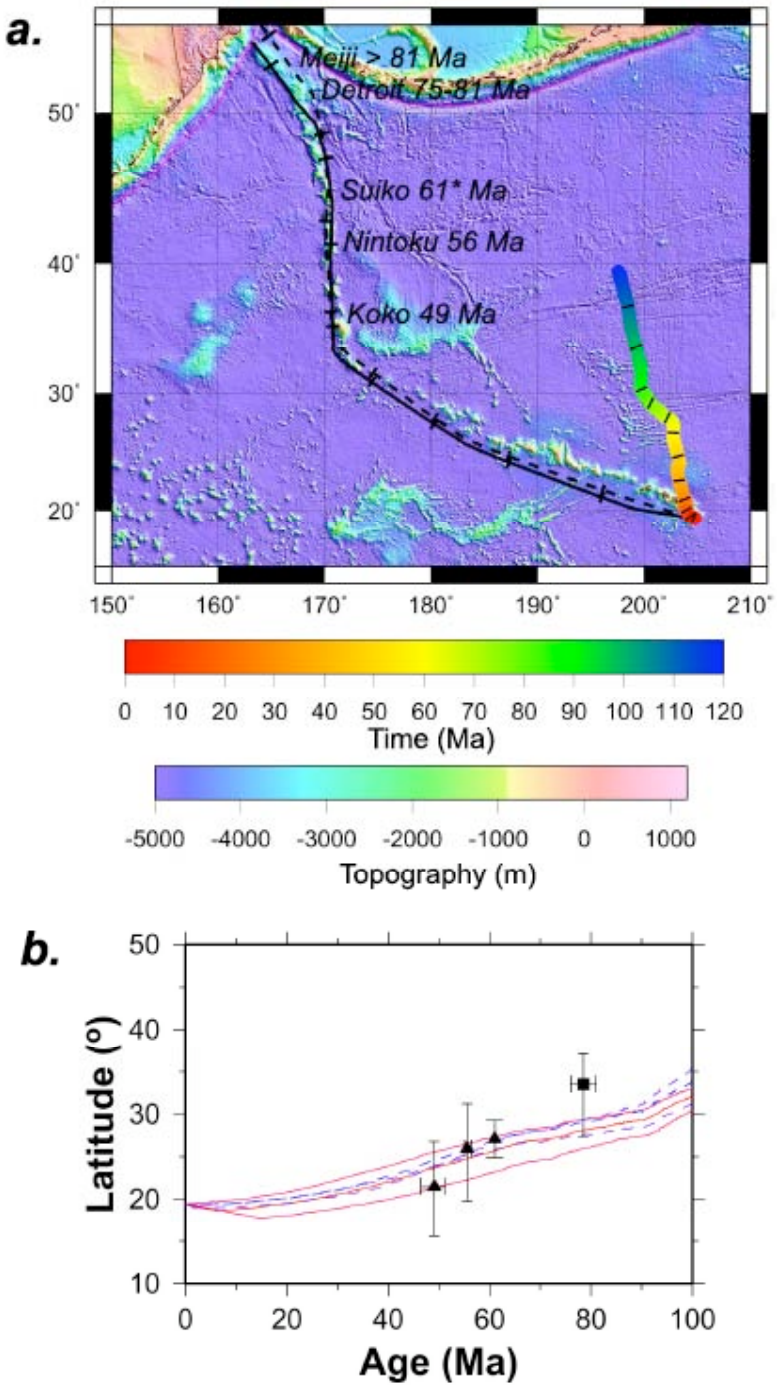


Figure 1. Comparison of geodynamic model results [Steinberger, 2000] and ODP Leg 197 paleomagnetic results. A. Computed Hawaiian hotspot motion for moving source model (colored line) and tracks for fixed source model (continuous line; plume initiation at 160 Ma) and moving source model (dashed line; plume initiation at 170 Ma). Tick marks are 10-m.y. increments. B. Computed changes of hotspot latitude for fixed source (continuous red lines) for plume initiation ages of 150, 160, and 170 Ma (upper to lower). Moving source model results (dashed lines) are shown for plume initiation at 180, 170, and 160 Ma (upper to lower). Paleolatitude means for Koko, Nintoku, Suiko and Detroit Seamounts (Model B, see text) are also shown. Asterix indicates revised age for Suiko Seamount [Sharp and Clague, 2006]. (After Tarduno et al., 2003).

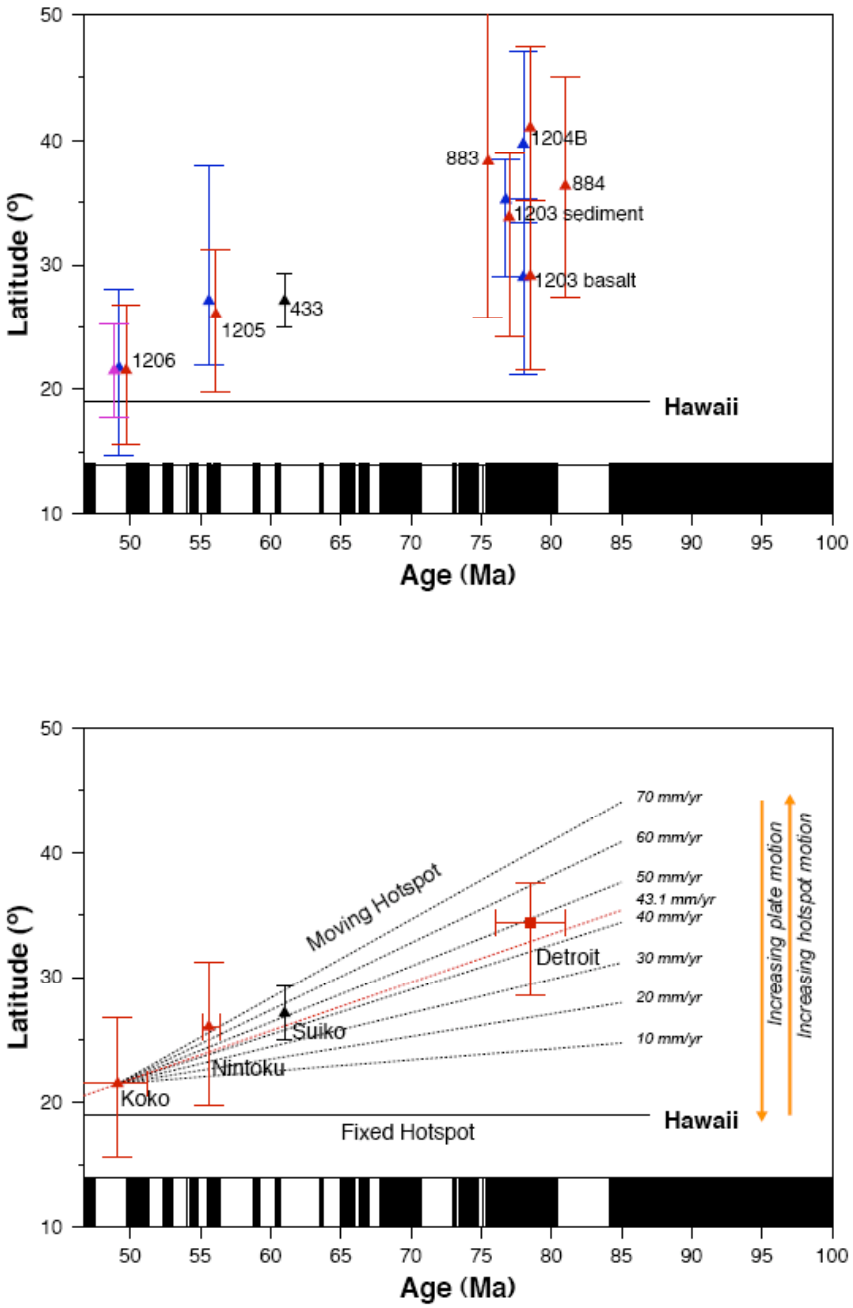


Figure 2. A. Paleolatitude data from ODP Leg 197 sites (1206, Koko Seamount; 1205, Nintoku Seamount; 1204B and 1203, Detroit Seamount), ODP Site 884 (Detroit Seamount; Tarduno and Cottrell, 1997), ODP Site 883 [Doubrovine and Tarduno, 2004], and DSDP Site 433 (Suiko Seamount; Kono, 1980). Red = results of thermal demagnetization; blue = results of alternating-field (AF) demagnetization. Result from Site 433 is based on AF and thermal data. Magenta = magnetization carried by hematite from weathered basalt from Site 1206. B. Average paleolatitude value for Detroit Seamount (square) based on inclination groups derived from basalts of Sites 884 and 1203 and Hole 1204B (see text) plotted with select paleolatitude values from other seamounts (see A). Also shown is a least-squares fit to the data (red) and several paleolatitude trajectories representing combinations of plate and hotspot motion. Geomagnetic polarity time scale of Cande and Kent [1995]. (After Tarduno et al., 2003).

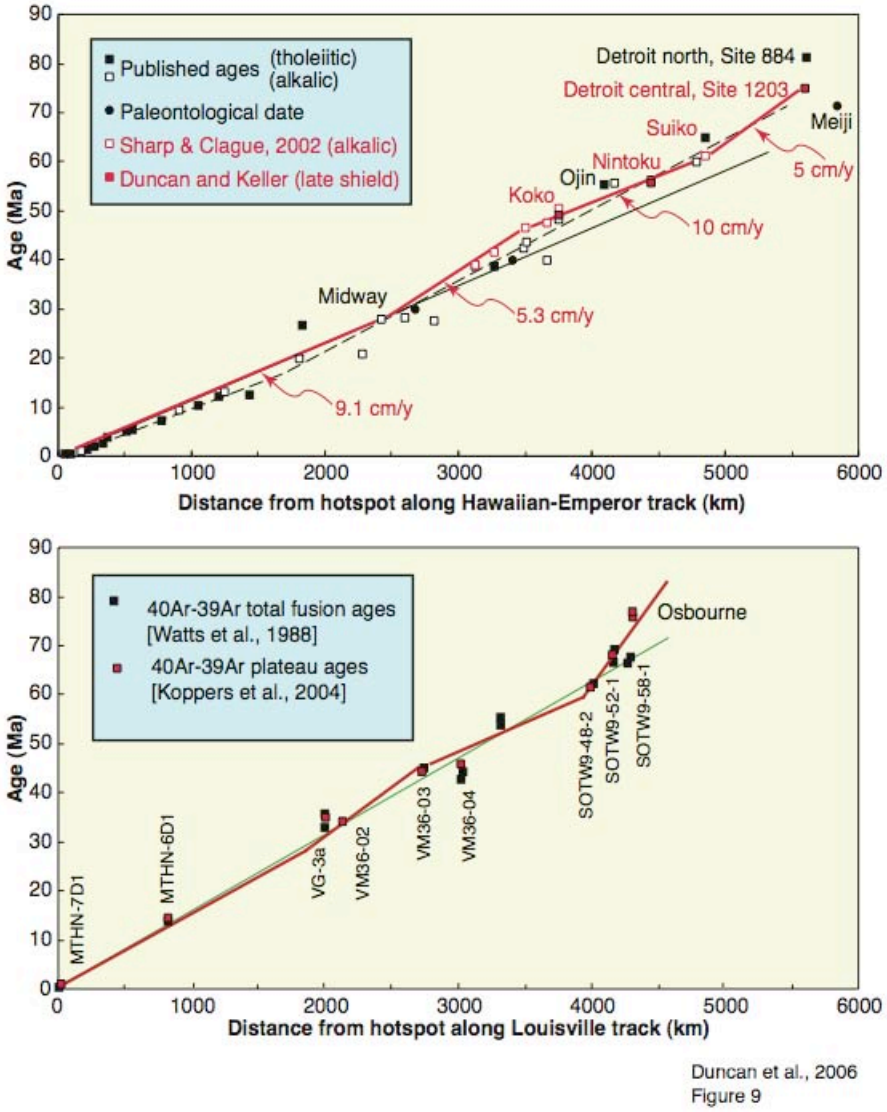


Figure 3. Age-distance relationship for Hawaiian-Emperor and Louisville volcanic chains. The latest, high-precision $^{40}Ar$-$^{39}Ar$ incremental heating ages appear to require changes in velocity for the Pacific plate, recorded in both chains.

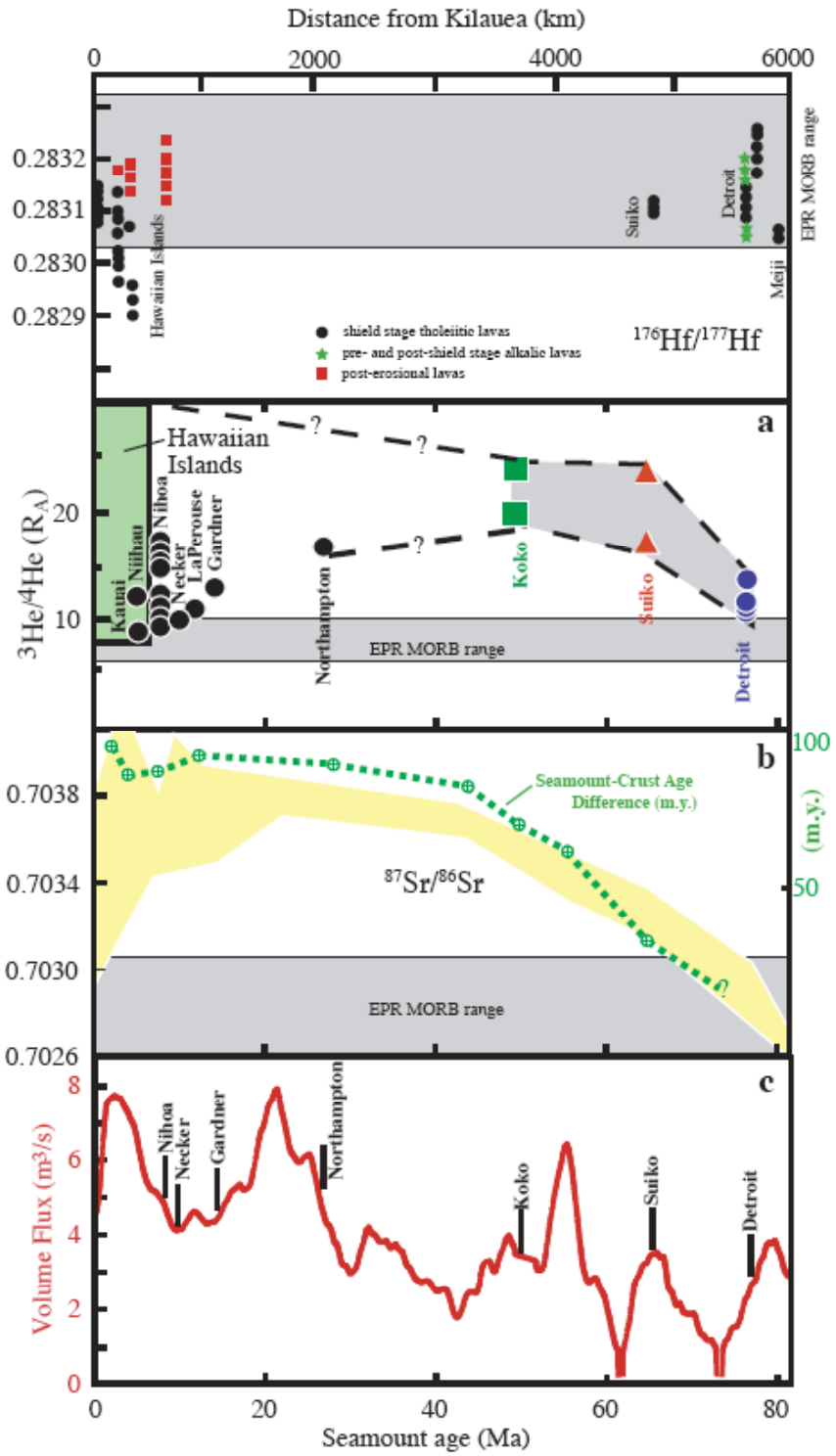


Figure 4. Isotopic variability along the Hawaiian-Emperor volcanic lineament (after Keller et al., 2004 and Frey et al., 2005). Hf-isotopic compositions indicate a persistent depleted component intrinsic to the plume. He-isotopic data are uniformly elevated relative to MORB, but decrease toward MORB values from Suiko to Detroit Seamounts. Sr-isotopic values show a progressive increase southward through the Emperor Seamounts, which is interpreted as decreasing partial mantle melting. No correlations are apparent between isotopic and magmatic volume variations (bottom panel).

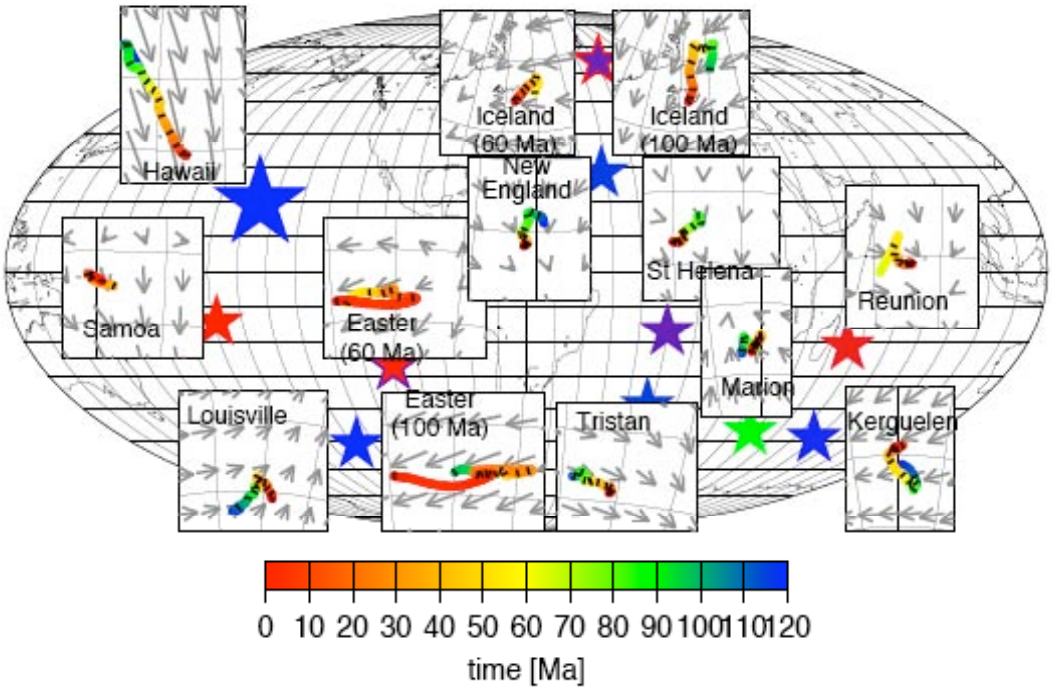


Figure 5. Computed hotspot motions with viscosity model 1 and temperature anomaly 500 K at plume base. Also included is the horizontal flow component at depth 933 km for Samoa, 1077 km for Easter and Iceland (60 Ma), 1220 km for Reunion, 1507 km for St. Helena, Easter and Iceland (100 Ma), 1651 km for Louisville, Tristan, New England and Kerguelen, 2081 km for Marion and Hawaii. These are approximately the depths from where plume conduit elements rose buoyantly since plume initiation time, and flow at these depths should approximate hotspot motion. Arrow length scale is 5 degrees of arc per cm/yr; grid spacing is 10 degrees here and in following figures. From Steinberger and Antretter (2006).

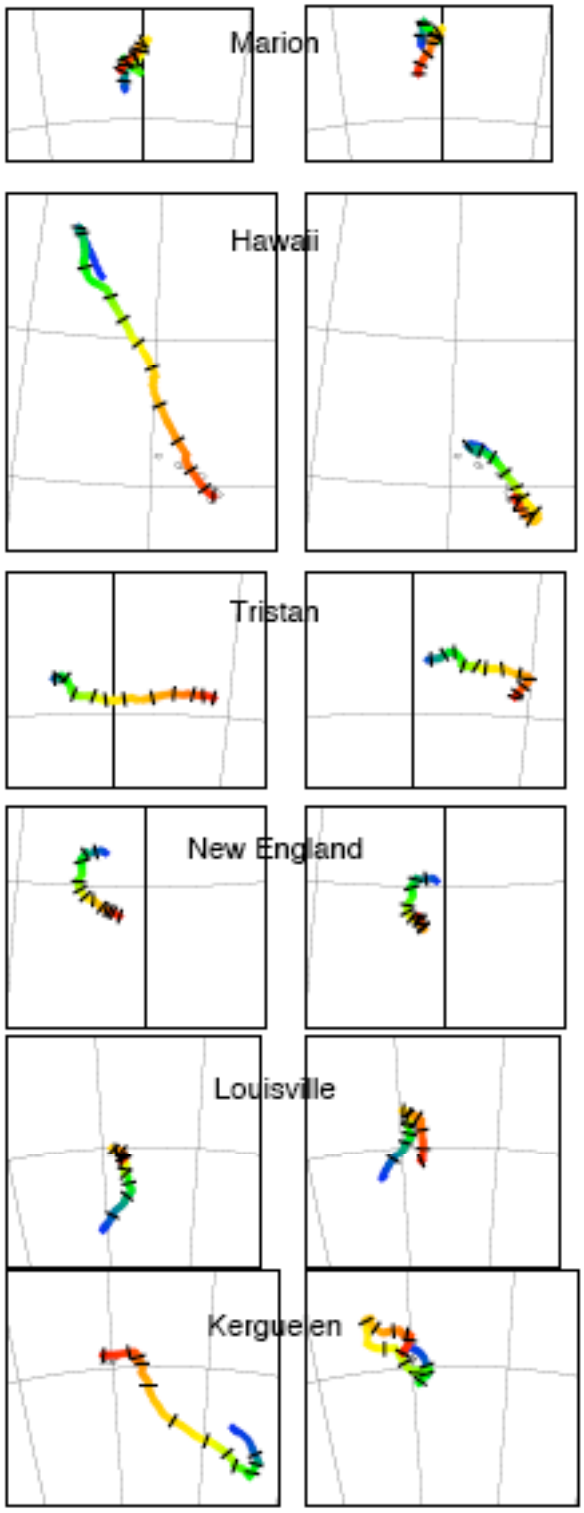


Figure 6. Computed hotspot motions with the same viscosity model as in Figure 5, but higher conduit rise speed of (1-10 cm/yr), with moving (left panels) and fixed (right panels) plume source. Color scheme as in Figure 5. From Steinberger and Antretter (2006).

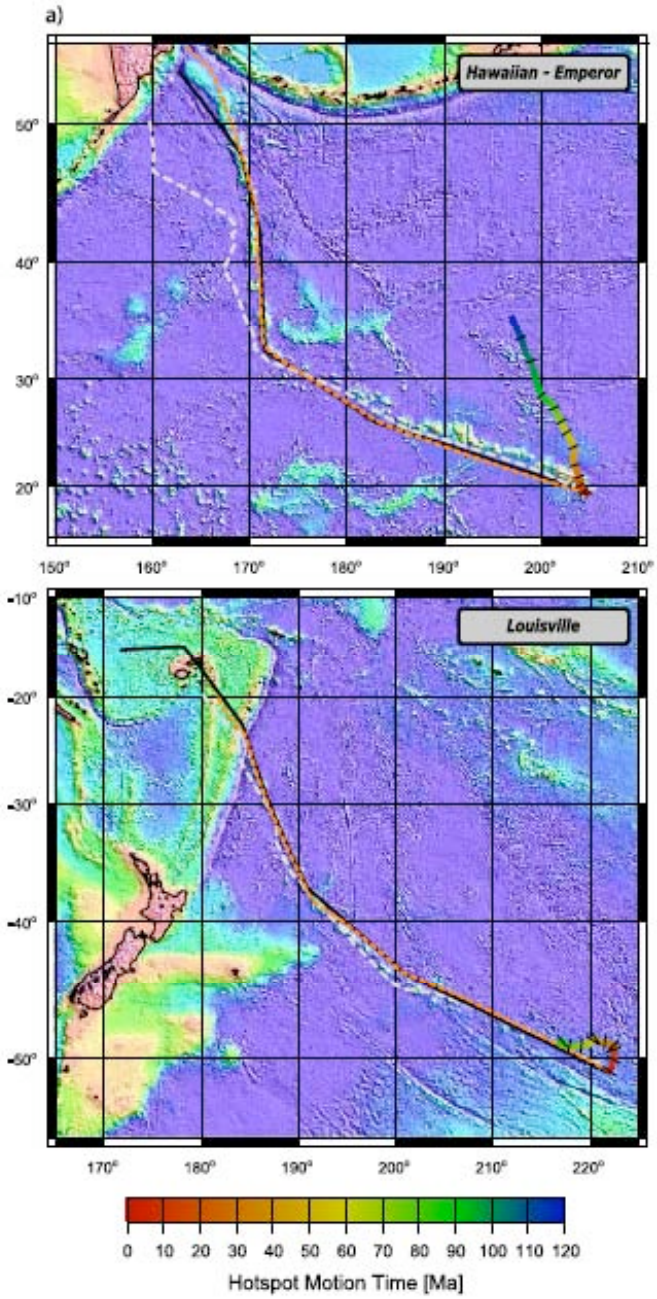


Figure 7. Computed hotspot motion and tracks for the Hawaiian and Louisville hotspots. Hotspot motion during the past 120 Ma is shown as rainbow-colored lines by the colored scale bar; tracks and age-distance relations are shown as single-colored lines for all cases discussed. Tick mark intervals are 10 Ma. Results are shown for the following models: Case [0] – black lines: fixed hotspots with best-fitting Pacific plate motion for four different rotations around the 0-25 Ma, 25-47 Ma, 47-62 Ma and 62-83 Ma stage poles; this model assumes a plume initiation age of 120 Ma for the Louisville hotspot. Case [1] – dashed orange lines: hotspot motion as in Steinberger et al. (2004) but a plume initiation age of 90 Ma for the Louisville hotspot. Best-fitting Pacific plate motion with the same time intervals as in Case 0. Case [2] – dashed gray lines: best fit to hotspot tracks in both hemispheres, with global plate motion model 2 of Steinberger et al. (2004) and four rotations of African plate for the same intervals as in Case 0.

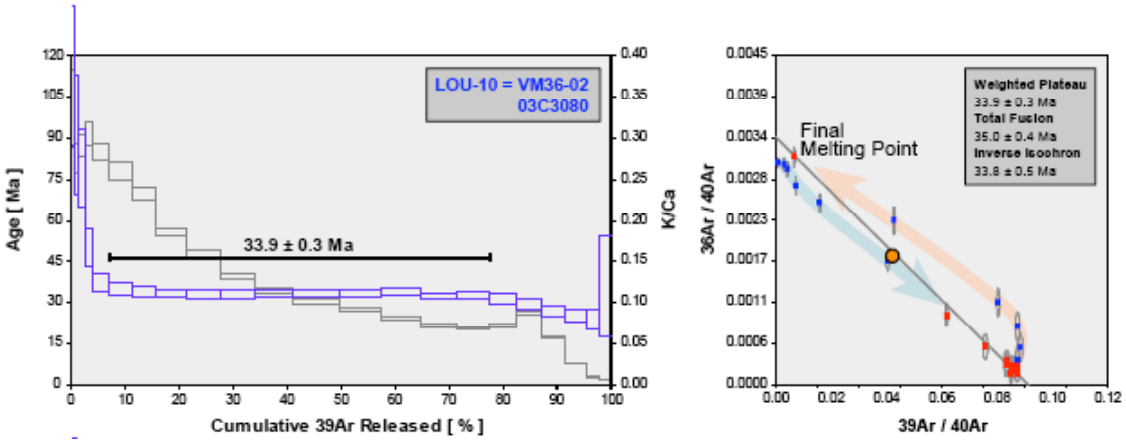


Figure 8. Typical degassing behavior in groundmass $^{40}Ar/^{39}Ar$ incremental heating analyses. In this representation, we display for each increment the fraction of the $^{36}Ar_{atm}$ and $^{37}Ar_{ca}$ and $^{38}Ar_{cl}$ components relative to the total amount of gas released during the experiment. These percentages have been normalized to the size of each degassing step, as approximated by the size of the $^{39}Ar_k$ component. Clear spikes are visible at the beginning and the end of each degassing spectra, reflecting the degassing of alteration products at low temperatures and high-Ca minerals, such as plagioclase and clinopyroxene, at high temperatures. From Koppers et al. (2004).

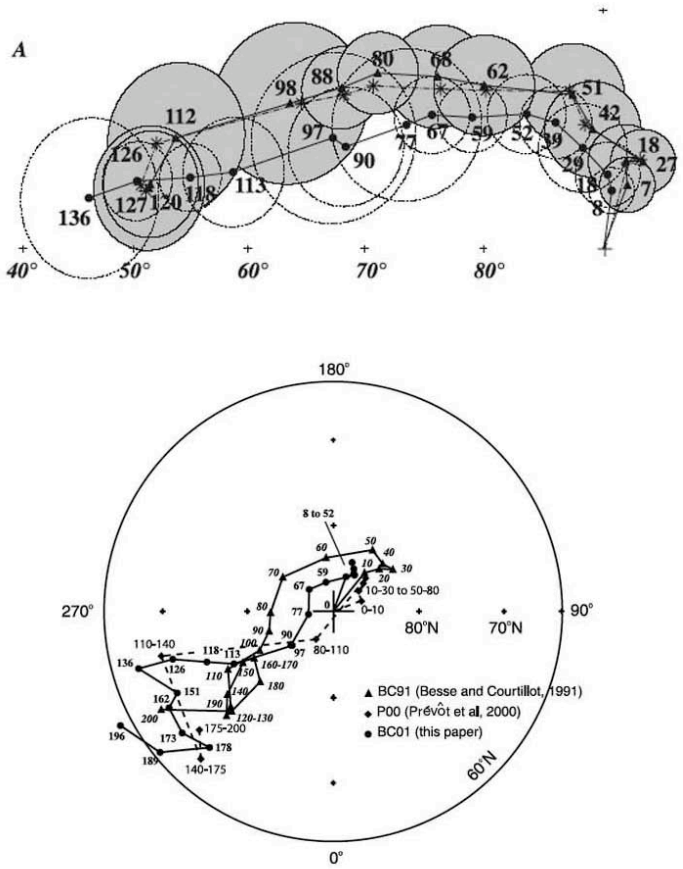


Figure 9. Example composite continental apparent polar wander paths. Top: Mid-Cretaceous to recent global APWP in South African plate coordinates. The cross at right is the spin axis. Triangles, asterisks, and filled circles are paleomagnetic poles with age labels in Ma. Triangles and asterisks show APWP from Besse and Courtillot (1991) whereas filled circles show updated analysis (Besse and Courtillot, 2002). Bottom: Composite APWP in the hotspot (mantle) reference frame, constructed by backtracking composite APWP at top using a model of African plate motion relative to the hotspots. Polar wander in this reference frame is sometimes interpreted as true polar wander. Three different paths are shown: triangles = Besse and Courtillot (1991); diamonds = Prévot et al (2000); circles = Besse and Courtillot (2002).

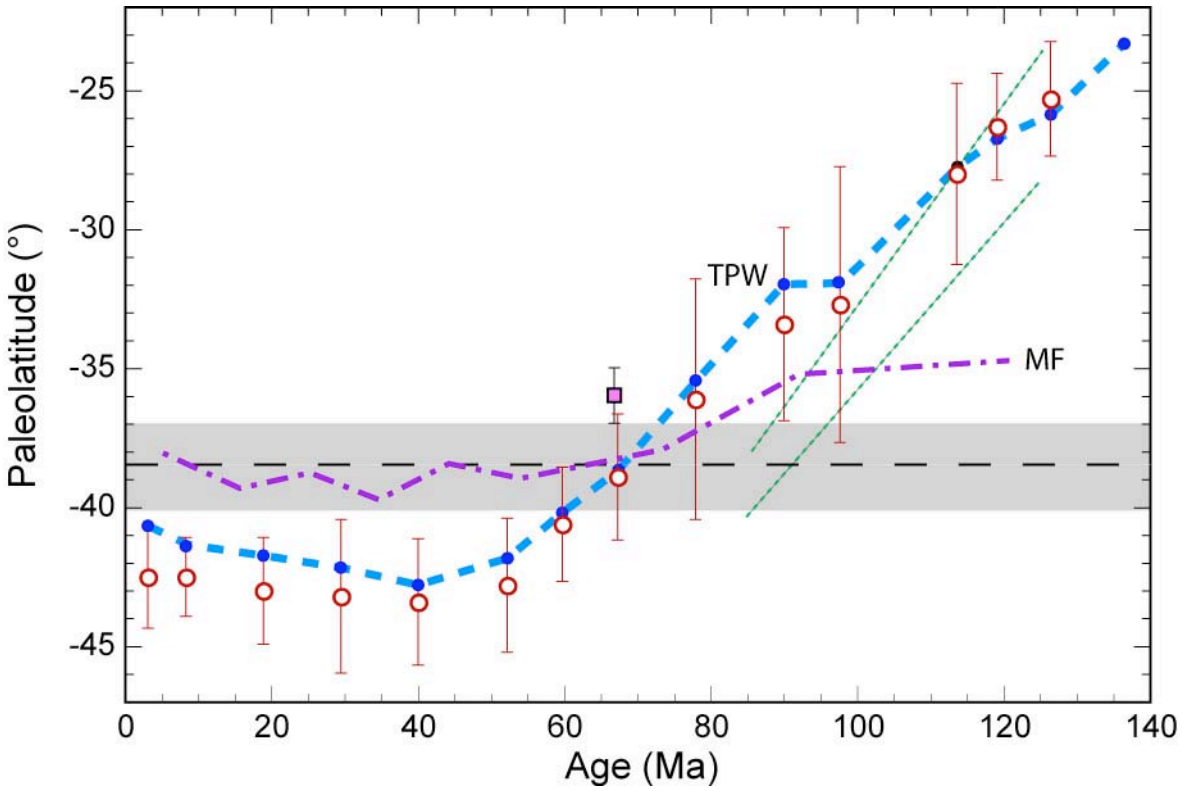


Figure 10. Paleolatitude estimates for Walvis Ridge (Tristan-Gough hotspot) from a global composite APWP. Open circles (red) show paleolatitude estimates calculated using the Besse and Courtillot (2002) polar path for South Africa and a model for hotspot propagation (O'Connor and LeRoex, 1992). Vertical bars show paleomagnetic 95% confidence limits. Heavy dashed line (blue; TPW) shows paleolatitude calculated from the Besse and Courtillot (2002) polar wander path in the mantle reference frame (which is very similar to the South Africa APWP). Dash-dot line (purple; MF) shows hotspot drift in paleolatitude from a mantle flow model (O'Neill et al., 2005). Thin dashed lines (green) show paleomagnetic estimate of hotspot paleolatitude change for the New England hotspot (van Fossen and Kent, 1992). Square (pink) is paleolatitude estimate from sedimentary paleomagnetic data from the Walvis Ridge (Chave, 1984). Gray band is latitude uncertainty of Tristan-Gough hotspot location (dashed line shows center of band).

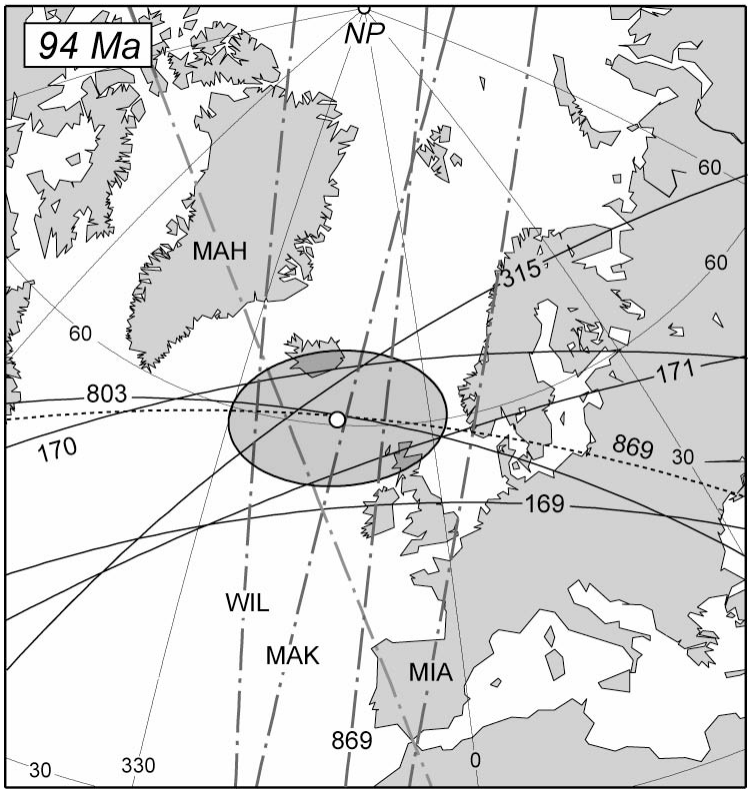


Figure 11. Example of mean paleomagnetic pole (average age 94 Ma) determined from a variety of data on the Pacific plate. Solid arcs define the locus of possible paleomagnetic poles constrained by basalt core paleolatitudes at various DSDP and ODP sites (labeled by site numbers). Dashed line is pole loci defined by sediment core from Site 869. Nearly vertical lines are loci of possible paleomagnetic poles defined by declination data from seamount magnetic anomaly models (WIL, MAK, MAH, MIA) and oriented sediments from Site 869. Mean pole is shown by open circle; ellipse shows 95% confidence region. From Sager (2007).

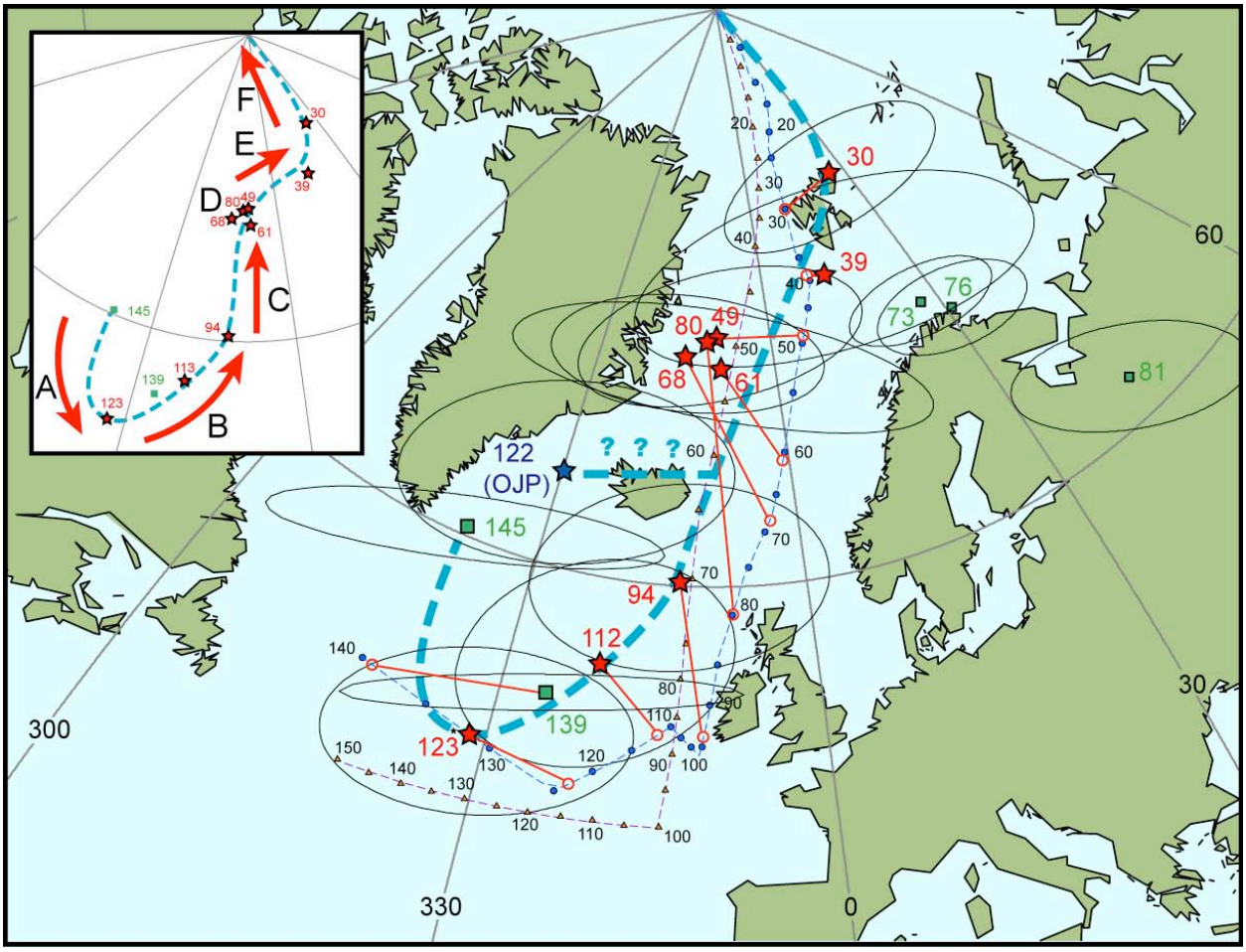


Figure 12. Pacific apparent polar wander path. Red stars denote pole positions defining the most likely APWP (Sager, 2006; Beaman et al., 2007), shown by the blue, heavy dashed line. Poles are surrounded by 95% confidence ellipses and labeled by age in Myr. Blue star denotes Ontong Java Plateau pole, which is considered anomalous (Sager, 2006). Green squares show poles determined from magnetic lineation skewness (73, 76, and 81 Ma poles from Petronotis and Gordon (1999), Vasas et al., (1994); 139 and 142 Ma poles from Larson and Sager (1992)). The Late Cretaceous skewness poles are considered anomalous (Beaman et al., 2007). Thin dashed lines show predicted polar wander path from plate/hotspot motion models of Duncan and Clague (1985) (purple with triangles) and Wessel et al. (2006) (blue with dots). Triangle and dot symbols show predicted pole positions at 5-Myr intervals, labeled every 10 Myr. Red lines show offset between paleomagnetic and hotspot model predicted poles. Inset sketch map shows interpreted phases of polar wander. Plot is an equal area map. Numbers are pole ages in Ma.

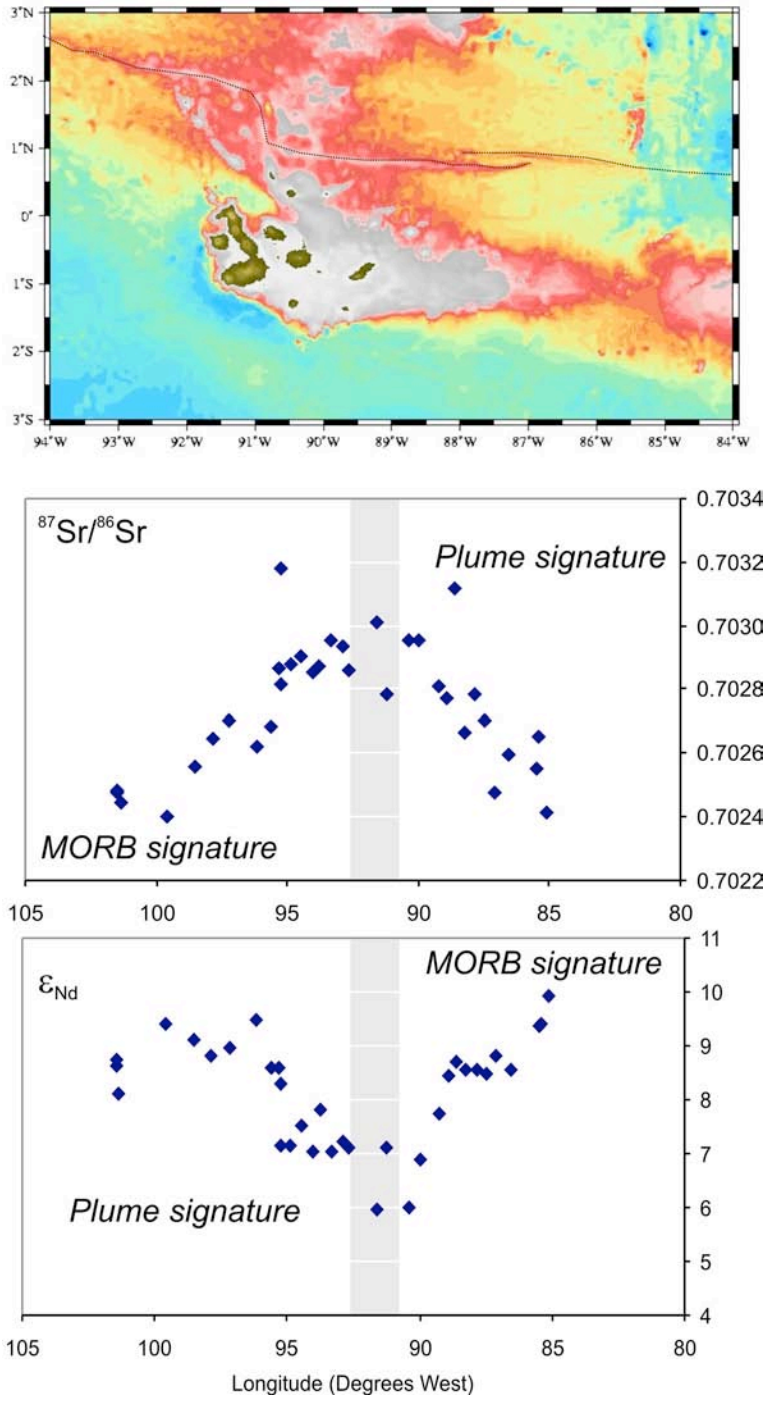


Figure 13. Radiogenic isotope ratios from along the Galapagos Spreading Center (data from Schilling et al., 2003). Shaded grey area represents the closest approach of the presumed Galapagos plume location to the GSC. In the top figure, the GSC is highlighted by a dashed line; bathymetric data from from W. Chadwick, pers. comm., http://newport.pmel.noaa.gov/~chadwick/Images/galap.final.jpg.

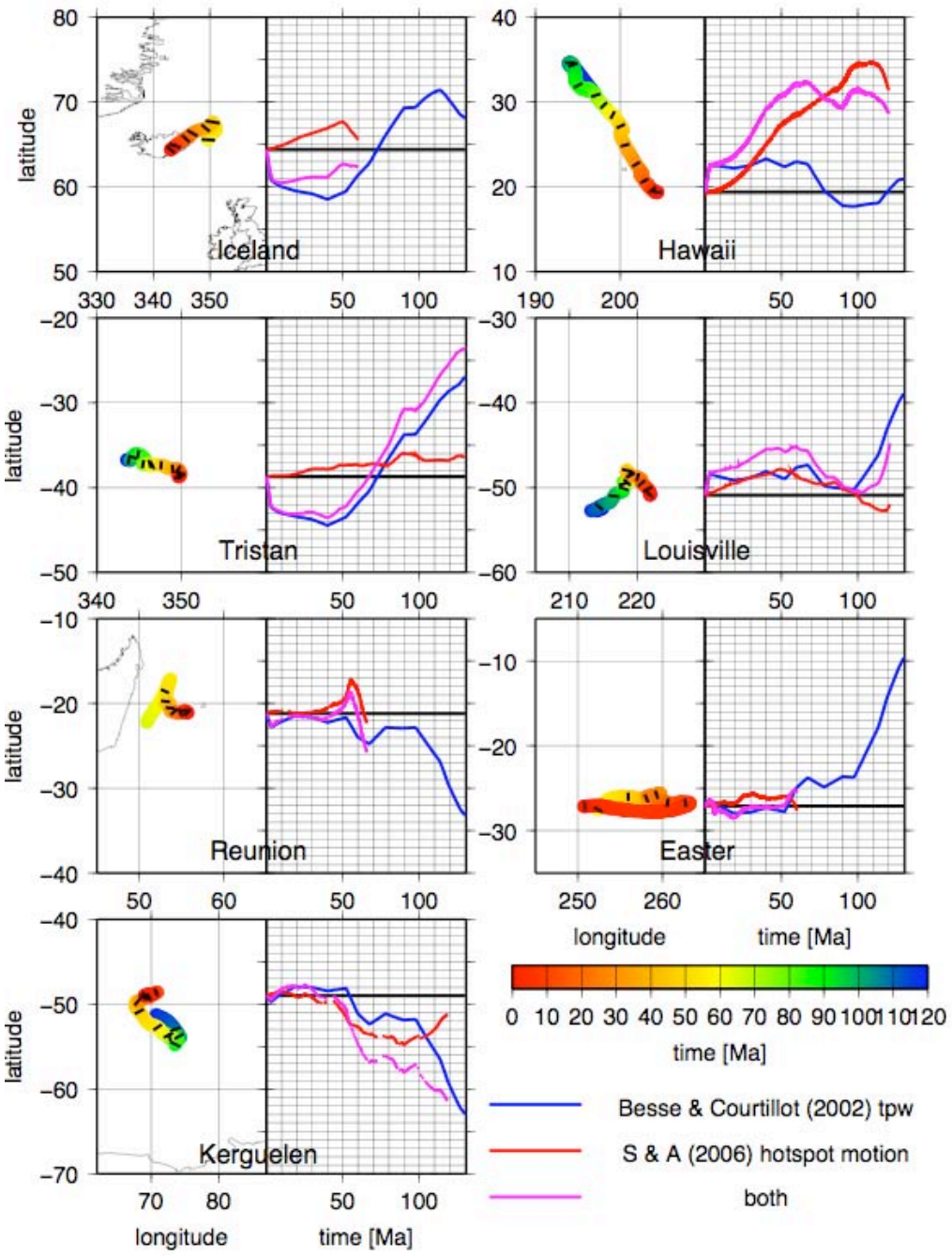


Figure 14. Predicted hotspot motion from mantle flow models ('worms' colored to show hotspot location with time, Steinberger and Antretter, 2006) and corresponding latitudinal motion (red lines in grids). Besse and Courtillot (2002) estimate of whole Earth motion with respect to the spin axis (true polar wander) derived from transferring the global continental APWP into a fixed hotspot reference frame yields a different prediction of latitudinal motion (blue lines in grids). The combination of these two effects is the purple lines in grids.

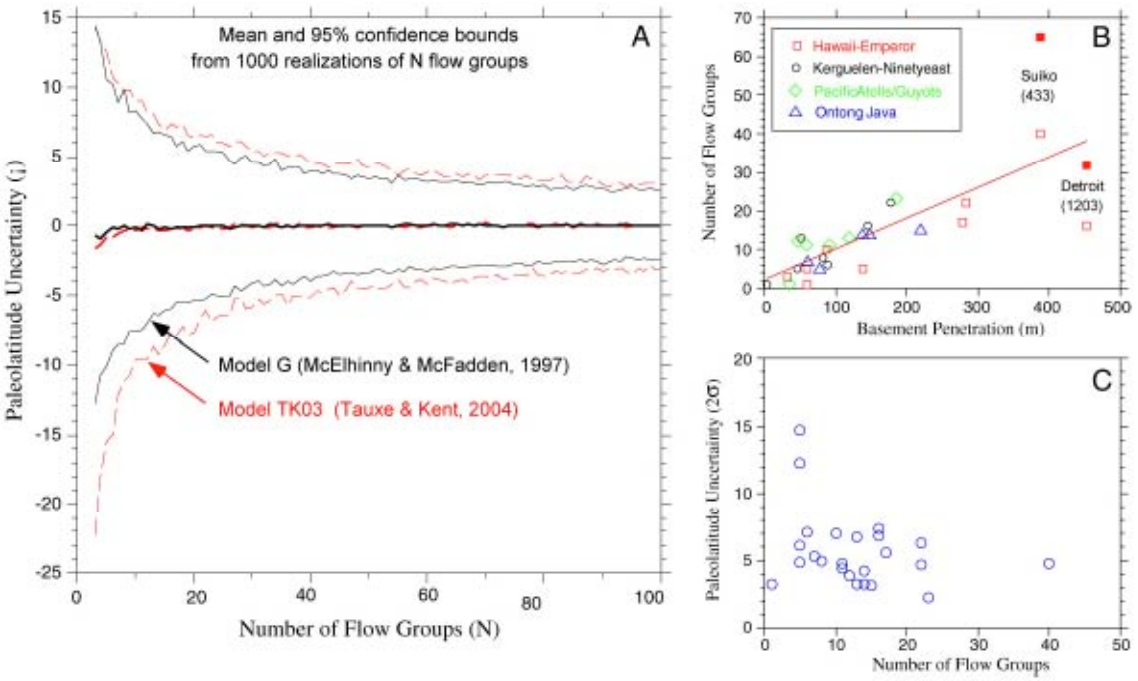


Figure 15. Paleosecular variation and paleolatitude uncertainties. **(a)** Mean and 95% paleolatitude uncertainties as a function of the number of temporally independent flow groups based on two recent paleosecular variation models. **(b)** Number of independent flow groups from selected DSDP/ODP sites. Hawaii-Emperor data from Leg 55 (Kono, 1980), 145 (Tarduno and Cottrell, 1997) and 197 (Tarduno et al., 2003). Filled squares for Suiko and Detroit indicate total number of flow units, including volcaniclastic units. Kerguelen-Ninetyeast Ridge data from Legs 120 (Inokuchi & Heider, 1992), 121 (Klootwijk et al., 1991) and 183 (Antretter et al., 2002). Pacific Atolls/Guyots data from Legs 143 (Tarduno & Sager, 1995) and 144 (Nakanishi and Gee, 1995). Ontong Java Plateau data from Legs 130 (Mayer and Tarduno, 1993) and 192 (Riisager et al., 2003). **(c)** Measured paleolatitude uncertainties as a function of number of flow groups for the data shown in (b).